AD-A071 834 GIANNOTTI AND BUCK ASSOCIATES INC RIVERDALE MD F/G 13/10
PREDICTION OF MOTIONS FOR THE T-AGOS HARD CHINE HULL.(U)
NOV 76 N00600-76-M-1803
UNCLASSIFIED NAVSEC-6136-76-39 NL

END
DATE FILMED
8-79
DDC

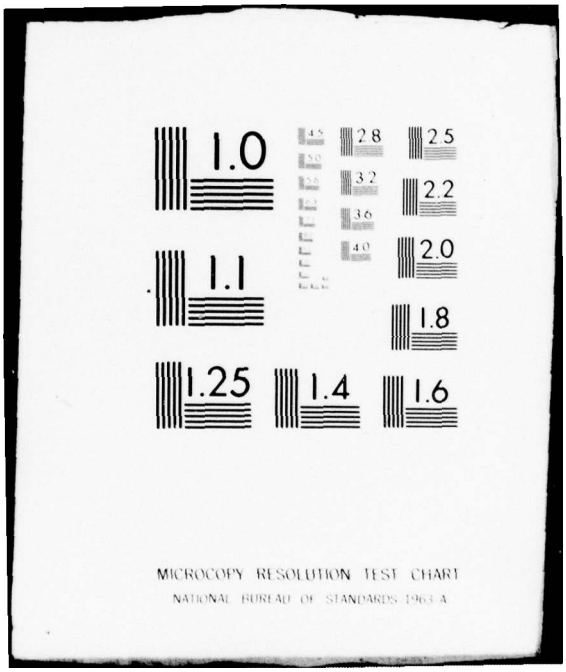
1.0
1.1
1.25
1.4
1.6
2.8
3.2
3.6
4.0
2.5
2.2
2.0
1.8
MICROCOPY RESOLUTION TEST CHART
NATIONAL BUREAU OF STANDARDS 1963-A

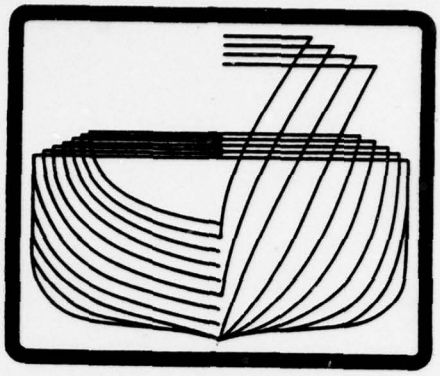

LEVEL II

PREDICTION OF MOTIONS FOR THE T-AGOS HARD CHINE HULL

NAVSEC REPORT 6136-76-39

9 NOVEMBER 1976

Prepared under the Technical
Direction of N. R. Fuller,

Hull Form and Fluid Dynamics Branch (Sec 6136)
Naval Ship Engineering Center
Hyattsville, Maryland 20782

by

Giannotti & Buck Associates, Inc.
5711 Sarvis Avenue, Suite 402
Riverdale, Maryland 20840

Under

Contract N00600-76-M-1803
(NAVSEC TPOC: N. R. Fuller)

Table of Contents

		Page
1.0	Scope and Objectives	1
2.0	The Five-Degree-of-Freedom Ship Motions Program	2
	2.1 Program Modifications	3
	2.2 Angular Motions	7
3.0	Results of Short-Term Predictions	10
4.0	Design Criteria Development	25
	4.1 Current State-of-the-Art	25
	4.2 Prediction of Long-Term Extreme Values	31
5.0	Design Criteria Recommendations	35
6.0	References	47
	Appendix I	48

LIST OF TABLES

TABLE NUMBER		PAGE
I	Comparison Between Experimental Results (Ref. 2) and the modified 5-DOF Motions Program Prediction	6
II	Results of Short Term Ship Motion Predictions	23
III	Results of Short Term Point Motion Predictions	24
IV	Standard Sea State Parameters	27
V	Roll Motions as a Function of Sea State	38

LIST OF FIGURES

FIGURE NUMBER		PAGE
1	Comparison of Non-Dimensional Roll Amplitudes Predicted by Experiment and MIT Five-Degree-of-Freedom Program	5
2	Sea State Characteristics	12
3(a)	Seaway Energy Spectrum	13
3(b)	Roll Response Amplitude Operator	13
3(c)	Roll Response Spectrum	13
4	Trends of Significant Heaving Motions with Significant Wave Height	14
5	Trends of Significant Pitching Motions with Significant Wave Height	15
6	Trends of Significant Rolling Motions with Significant Wave Height	16
7	Trends of Angular and Tangential Velocity in Roll	18
8	Trends of Angular and Tangential Acceleration in Roll	19
9	Trends of Normal Acceleration in Roll	20
10	Trends of Vertical Motions at Point 4	21
11	Characteristics of Ocean Waves	28
12	SES-100B Data Plotted on Weibull Distribution Paper	30
13	Weibull Cumulative Distribution of x/x_{rms}	34
14	Long-Term Distribution of Roll Amplitude	41
15	Long-Term Distribution of Roll Velocity	42

LIST OF FIGURES (Con't.)

FIGURE NUMBER		PAGE
16	Long-Term Distribution of Roll Acceleration	43
17	Long-Term Distribution of Tangential Velocity at R = 82.83 ft.	44
18	Long-Term Distribution of Tangential Acceleration at 82.83 ft.	45
19	Long-Term Distribution of Normal Acceleration at R = 82.83 ft.	46
I.1	Characteristics of the Generalized Gamma Distribution	49
I.2	The Weibull Probability Density Function	51
I.3	The Weibull Cumulative Probability for a Range of Values of c	52
I.4	The Weibull Cumulative Probability Plotted on Semi-log Graph Paper	53
I.5	Definition of "Average of Highest 1/b values of x"	54
I.6	Characteristics of the Weibull Distribution	56
I.7	Characteristics of the Weibull Distribution	57

1.0 Scope and Objectives

Giannotti and Buck Associates, Inc. has been tasked by the Naval Ship Engineering Center, Code 6136, to perform motion analyses on an oceanographic and research survey ship, T-AGOS, now in the concept design stage. Of particular interest in the study are two points on the ship representing equipment interface locations. The first point is located at Frame 59 on ship with three alternate heights having been investigated. The second point is located on the upper side of the cap rail on the fantail bulwark. The primary vehicle used in the analysis is the Five-Degree-of-Freedom Ship Motions Computer Program maintained by NAVSEC Code 6136. Statistical characteristics of the motions and long term motion predictions were desired. This report presents the approach to the problem and reports the results of the analyses.

2.0 The Five-Degree-of-Freedom Ship Motions Program

The basic 5-DOF Program predicts ship response in five degrees of freedom (surge neglected) and was developed under the supervision of Dr. C. Chryssostomidis of MIT using the theory presented by Salvesen, Tuck and Faltinsen (1). For the purpose of calculating the various hydrodynamic coefficients used in the program the

ship sections are represented by so called Lewis-forms. These are ship-like sectional shapes, completely fair, without chines, knuckles or discontinuities and are obtained by a conformal mapping technique using local section beam, draft and area as arguments. The difficulties introduced in representing a double chine hull with this form will be discussed in the next section.

The program contains several options for seaway representation. In addition to regular wave responses at any heading in waves of any length, heights, or slope, long crested unidirectional irregular waves may be introduced having spectral characteristics either of the standard Pierson-Moskowitz spectrum or of any desired input spectrum. The Pierson-Moskowitz spectrum is usually used for representation of a fully developed storm seas of long duration but such seas occur less frequently in nature than do partially developed seas of shorter duration. Seas of this type are better represented by the Bretsneider two parameter spectrum. As a third alternative, wave spectra based on direct observation rather than mathematical modeling can be introduced.

For the purposes of this study the Pierson-Moskowitz spectrum was used throughout.

The program computes absolute and relative <u>vertical</u> motions amplitudes, velocities, and accelerations and <u>transverse</u> accelerations only at any point specified.

In its basic form the program also predicts hull bending moments, torsional moments and shear forces generated dynamically in waves.

In addition, the occurrence and frequency of deck wetness, slamming, and propeller racing may be forecast although none of these features were used in this study.

A modification to the original program permits the introduction of experimentally determined Response Amplitude Operators, a feature which was invoked in this study.

2.1 Program Modifications

An experimental study of several round bilge and hard chine hull forms, including the T-AGOS parent hull form has been conducted by Sibul (2) at the University of California. Sibul compared the resistances of the hulls in calm water and their motions in head and beam seas. Past experience has indicated that analytical ship motions programs give generally good results in predicting the smaller motions-pitch, heave, yaw and sway--but rolling motion, because of its usually large amplitude and non-linear character, is more difficult. In this case the difficulty is compounded by the fact that the hard chines are not well modeled by the Lewis-form representation. As Sibul showed experimentally the hard chines have a substantial effect in damping rolling motions.

The 5-DOF Program contains a feature which permits the simultation of bilge keels in the representation. Since these

appendages have a generally similar effect to the sharp corners of the hard chine hull some initial computer runs were made in an attempt to duplicate the experimental evidence using bilge keels to simulate the chines. Figure 1 shows the results of several of these attempts compared to the Sibul data. The ordinate of these curves is roll amplitude divided by wave slope. As the waves become very long, that is as the frequency goes to zero, the response should be just equal to the forcing function. In other words, the non-dimensionalized rolling motion should approach unity. As indicated in Figure 1 the modified 5-DOF Program does not predict this, a fact which casts a shadow on the value of the roll predictions made by the program. The fault could be either in the theory or in the way the theory is programmed. It will take further study to determine the precise cause and correct it. In the meantime, efforts to use the analytical roll prediction for this application were abandoned and the Sibul experimental roll operators were introduced in the program. Analytically calculated operators in the other modes of motion were continued.

In Table 1 Sibul's experimental results are reproduced together with the predictions made by the modified 5-DOF Program. As Table I shows, the modified Program using analytically determined operators in pitch and heave and experimentally determined operators in roll slightly overpredicts in pitch, underpredicts in heave and underpredicts in roll. Although the agreement is not impressive it is reasonable considering differences in the experimental and theoretical input wave spectrum.

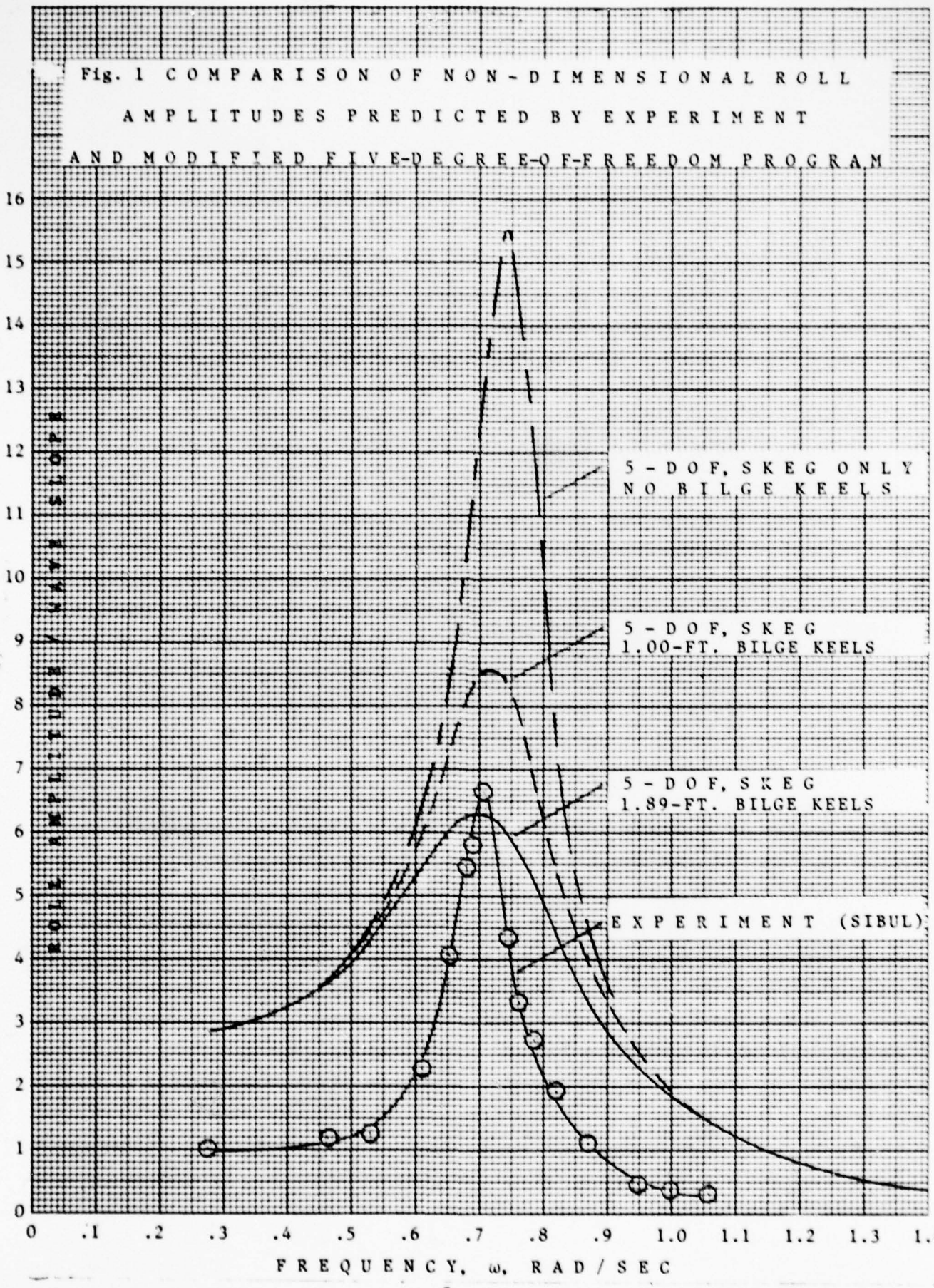
Fig. 1 COMPARISON OF NON-DIMENSIONAL ROLL AMPLITUDES PREDICTED BY EXPERIMENT AND MODIFIED FIVE-DEGREE-OF-FREEDOM PROGRAM
5 - DOF, SKEG ONLY NO BILGE KEELS
5 - DOF, SKEG 1.00-FT. BILGE KEELS
5 - DOF, SKEG 1.89-FT. BILGE KEELS
EXPERIMENT (SIBUL)
0
1
2
3
4
5
6
7
8
9
10
11
12
13
14
15
16
0 .1 .2 .3 .4 .5 .6 .7 .8 .9 1.0 1.1 1.2 1.3 1.4
FREQUENCY, ω, RAD/SEC

TABLE I

Comparison Between Experimental Results (Ref. 2) and the Modified 5-DOF Motions Program Prediction

			← SIBUL →		← MODIFIED 5 DOF →	
Mode	Heading	Speed, kts.	Sig. Wave ht.	Dbl. Amp.	Sig. Wave Ht.	Dbl. Amp.
Pitch, deg.	Head Seas	3.0	8.64	7.64	8.64	7.87(1)
Heave, ft.	Head Seas	3.0	8.64	6.19	8.64	4.44(1)
Roll, deg.	Beam Seas	0.0	9.60	31.8	10.20	26.5(2)

(1) Using analytically predicted RAO with 1.0' bilge keel width.

(2) Using RAO determined experimentally in regular wave tests.

2.2 Angular Motions

Motions at specified points are of special interest in this study in that these points are candidate equipment interface locations. The coordinate system and the locations of the specified points are shown below.

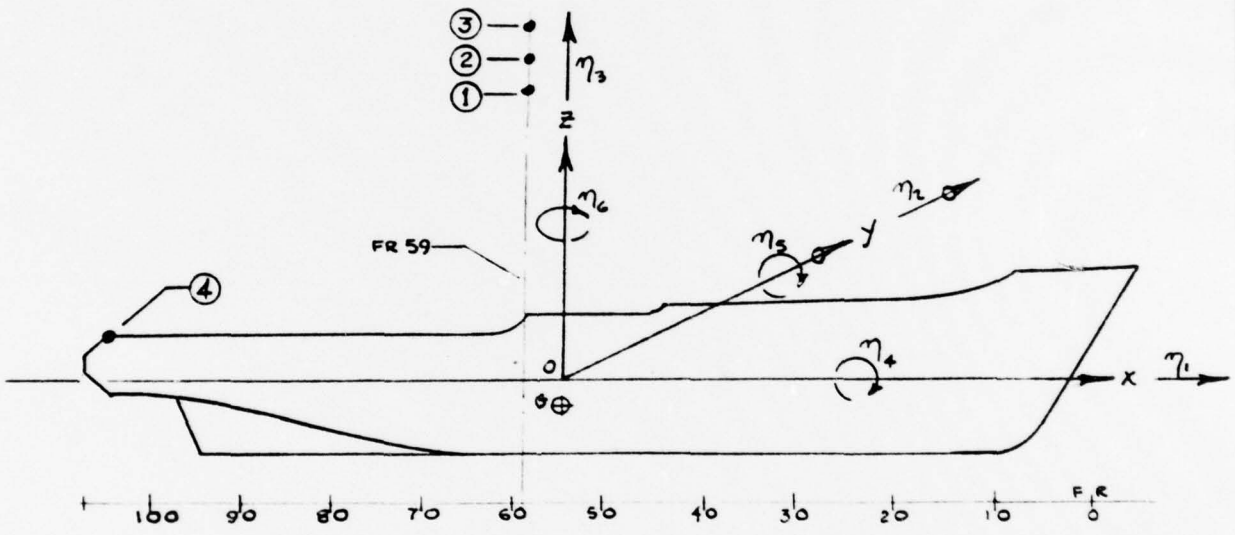

The origin of the (x,y,z) coordinate system is fixed with respect to the mean position of the ship in the undisturbed free surface with the z-axis vertically upward through the center of gravity. The translational displacements in the x,y,z directions are η_1, η_2, and η_3. The rotational displacements about the x,y, and z axes are η_4, η_5, and η_6.

Thus,

η_1 = surge	η_4 = roll
η_2 = sway	η_5 = pitch
η_3 = heave	η_6 = yaw

The locations of the specified points of interest are:

	x	y	z
Point 1	-5.84	0.0	64.00
Point 2	-5.84	0.0	70.63
Point 3	-5.84	0.0	77.25
Point 4	-102.84	0.0	9.25

Points 1, 2, and 3 are three alternate heights of a sensor to be located at Frame 59. Point 4 is located on the cap rail of the fantail bulwark.

As noted the program computes absolute and relative vertical motions, amplitudes, velocities and accelerations and transverse accelerations only at specified points. In the basic MIT program this feature computed correctly; however, in the version that accommodates externally generated RAO's there is an error in the program which has not as of this time been identified although the other features of the program compute correctly. Considering the nature of the equipment involved, the vertical and transverse motions are primarily of interest at Point 4 and for this purpose

the predictions generated by the basic program are considered satisfactory.

For the equipment to be located at Points 1, 2, or 3 the angular displacements, maximum angular velocities, maximum angular accelerations, and maximum x,y,z components of linear velocity and acceleration at the location of the point are of greater interest. An attempt was made to introduce computation of these elements into the external RAO version of the program. Within the time and cost constraints of this study the attempt was not successful and was deferred to a later effort. To produce useful and timely answers hand calculation was resorted to for a limited number of the most significant cases. Since rolling motions are of largest magnitude the maximum values in the roll mode of angular velocity, angular acceleration, tangential velocity (linear y-component at the point), tangential acceleration (linear y-component at the point), and normal acceleration (linear z-component at the point) were computed by hand. These values were also computed for the worst case in the pitch mode to give a comparison of magnitudes.

The computational relationships involved in calculating the angular motions are given below.

Maximum angular velocity:

$$\dot{\eta}_{i_{max}} = \omega_e \eta_{i_{max}} \quad , \; i = 4,5,6$$

Maximum angular acceleration:

$$\ddot{\eta}_{i_{max}} = \omega_e^2 \eta_{i_{max}}$$
$$= \omega_e \dot{\eta}_{i_{max}}$$

Maximum tangential velocity: $v_t = R_k \dot{\eta}_{i_{max}}$

Maximum tangential acceleration: $a_t = R_k \ddot{\eta}_{i_{max}}$

Maximum normal acceleration:

$$a_n = R_k (\dot{\eta}_{i_{max}})^2$$
$$= R_k \eta_{i_{max}} \ddot{\eta}_{i_{max}}$$

Here, ω_e = frequency of encounter

$$= \omega(1-\omega \frac{v_s \cos \alpha}{g})$$

v_s = ship speed, ft/sec

α = heading angle

R_k = projected radius from ship c.g. to k^{th} point in plane normal to motion axis.

In our case $R_k = Z_k + OG = Z_k + 5.58'$

Point 1: $R_1 = 69.58$

Point 2: $R_2 = 76.21$

Point 3: $R_3 = 82.83$

Note that if values of tangential velocity and acceleration and normal acceleration are given for one point, values at other points may be determined by simple ratio.

3.0 Results of Short Term Predictions

The predictions cited in this section are all for irregular long crested seas using the Pierson-Moskowitz Spectrum. Significant

wave heights used to represent the various Sea States are shown in Figure 2 which is a graphical display of the traditional table of Wind and Sea Scales due to Wilbur Marks.

Three headings--head seas (180^{o}), bow seas (135^{o}) and beam seas (90^{o}), and three speeds, 0, 3, and 5 knots--were addressed in the study.

Roll is the dominant mode of motion in the seakeeping performance of the T-AGOS design, and the mode which primarily drives the motions of Points 1, 2, and 3. Figure 3 illustrates the interaction of the ship in the roll mode and the fully developed seaways. The usual operator approach is employed:

Seaway Energy Spectrum, $S_{\zeta}(\omega)$ x Ship Response Amplitude Operator, $Y_{\eta_4}(\omega)$ = Ship Response Spectrum, $S_{\eta_4}(\omega)$.

Note the sharply tuned character of the Roll RAO. Because of this feature the ship does not respond to much of the huge blocks of energy in the State 6 and State 7 Sea States. Any reduction in the Metacentric Height (GM) during the design process will cause the ship to roll at a lower natural frequency thus shifting the RAO to the left thus producing much larger rolling motions and much larger motions at Points 1, 2, and 3.

The significant heaving, pitching, and rolling motions, that is the average of the 1/3 highest motions, are displayed in Figures 4, 5, and 6. Heaving motions will drive the motion of Point 4 on the fantail. Figure 4 shows that these motions are

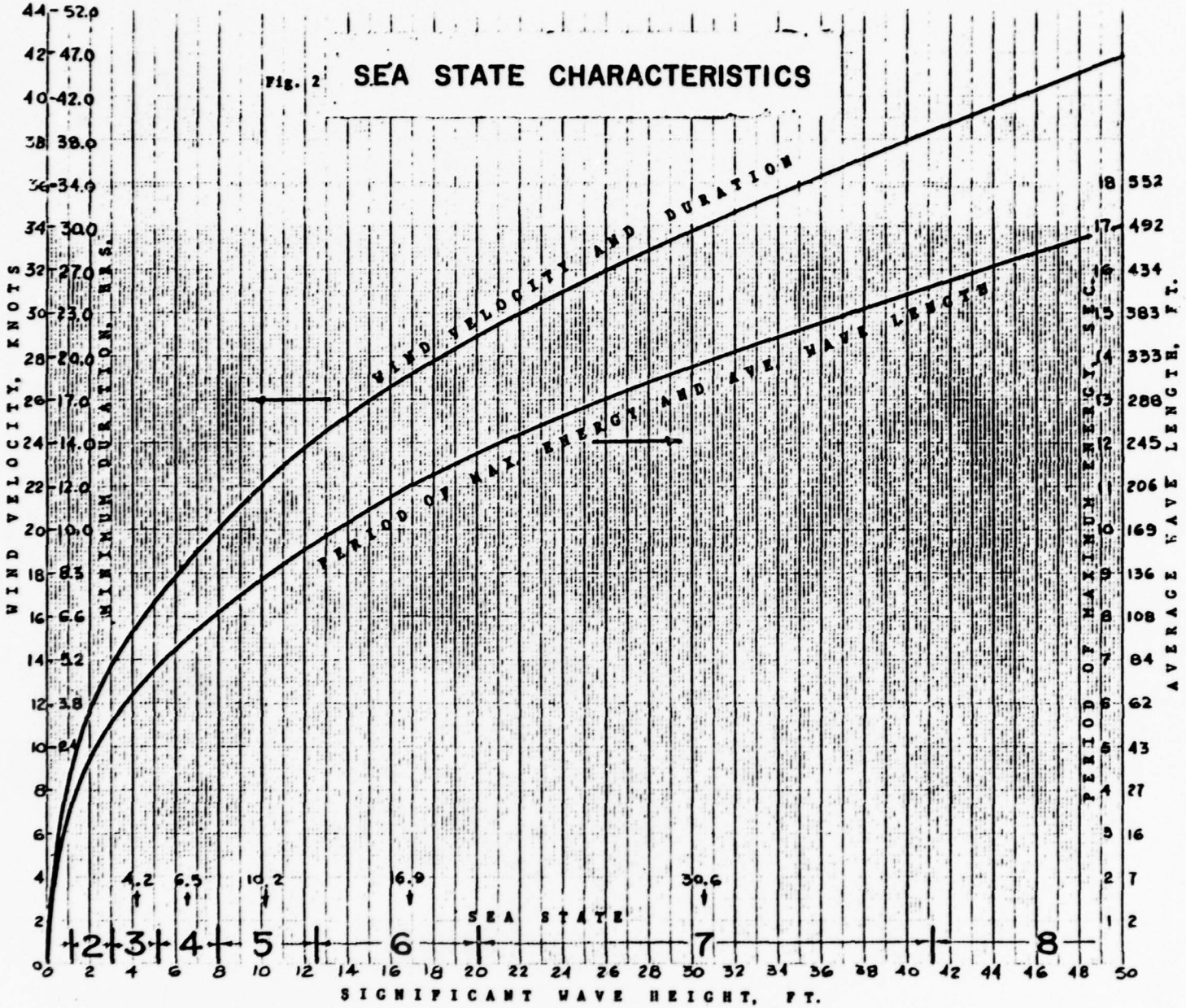
SEA STATE CHARACTERISTICS
WIND VELOCITY, KNOTS
MINIMUM DURATION, HRS.
WIND VELOCITY AND DURATION
PERIOD OF MAX. ENERGY AND AVE WAVE LENGTH
PERIOD OF MAXIMUM ENERGY, SEC.
AVERAGE WAVE LENGTH, FT.
SEA STATE
SIGNIFICANT WAVE HEIGHT, FT.
4.2
6.5
10.2
16.9
30.6

Fig. 2

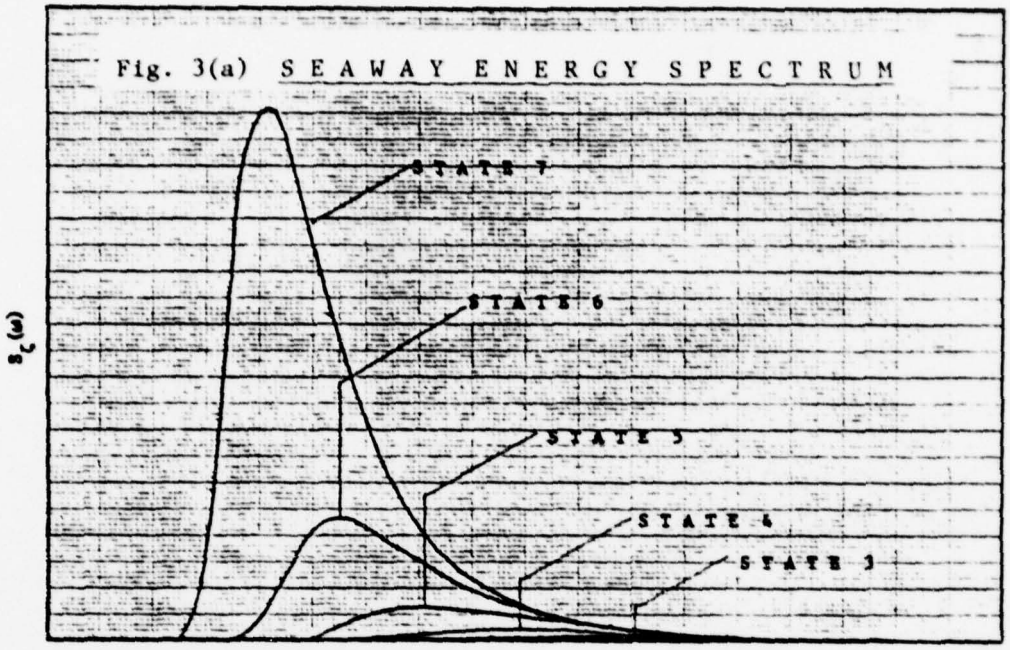
Fig. 3(a) SEAWAY ENERGY SPECTRUM
STATE 7
STATE 6
STATE 5
STATE 4
STATE 3
$S_\zeta(\omega)$

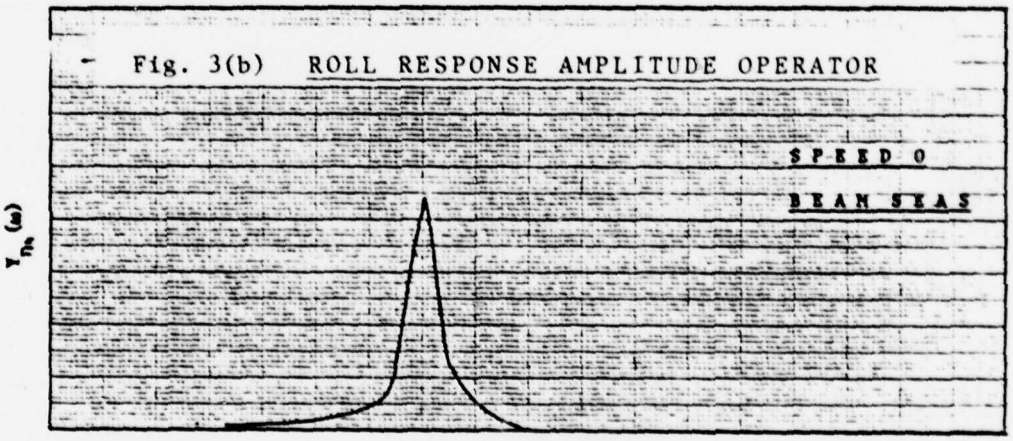
Fig. 3(b) ROLL RESPONSE AMPLITUDE OPERATOR
SPEED 0
BEAM SEAS
$Y_{\eta_4}(\omega)$

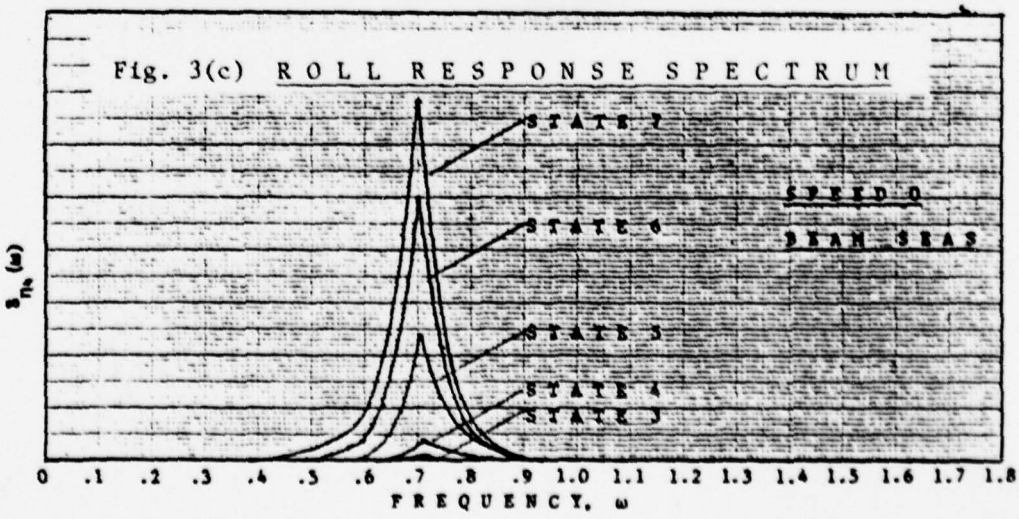
Fig. 3(c) ROLL RESPONSE SPECTRUM
STATE 7
STATE 6
STATE 5
STATE 4
STATE 3
SPEED 0
BEAM SEAS
$S_{\eta_4}(\omega)$
0 .1 .2 .3 .4 .5 .6 .7 .8 .9 1.0 1.1 1.2 1.3 1.4 1.5 1.6 1.7 1.8
FREQUENCY, ω

Fig. 4 TRENDS OF SIGNIFICANT HEAVING MOTIONS WITH SIGNIFICANT WAVE HEIGHT

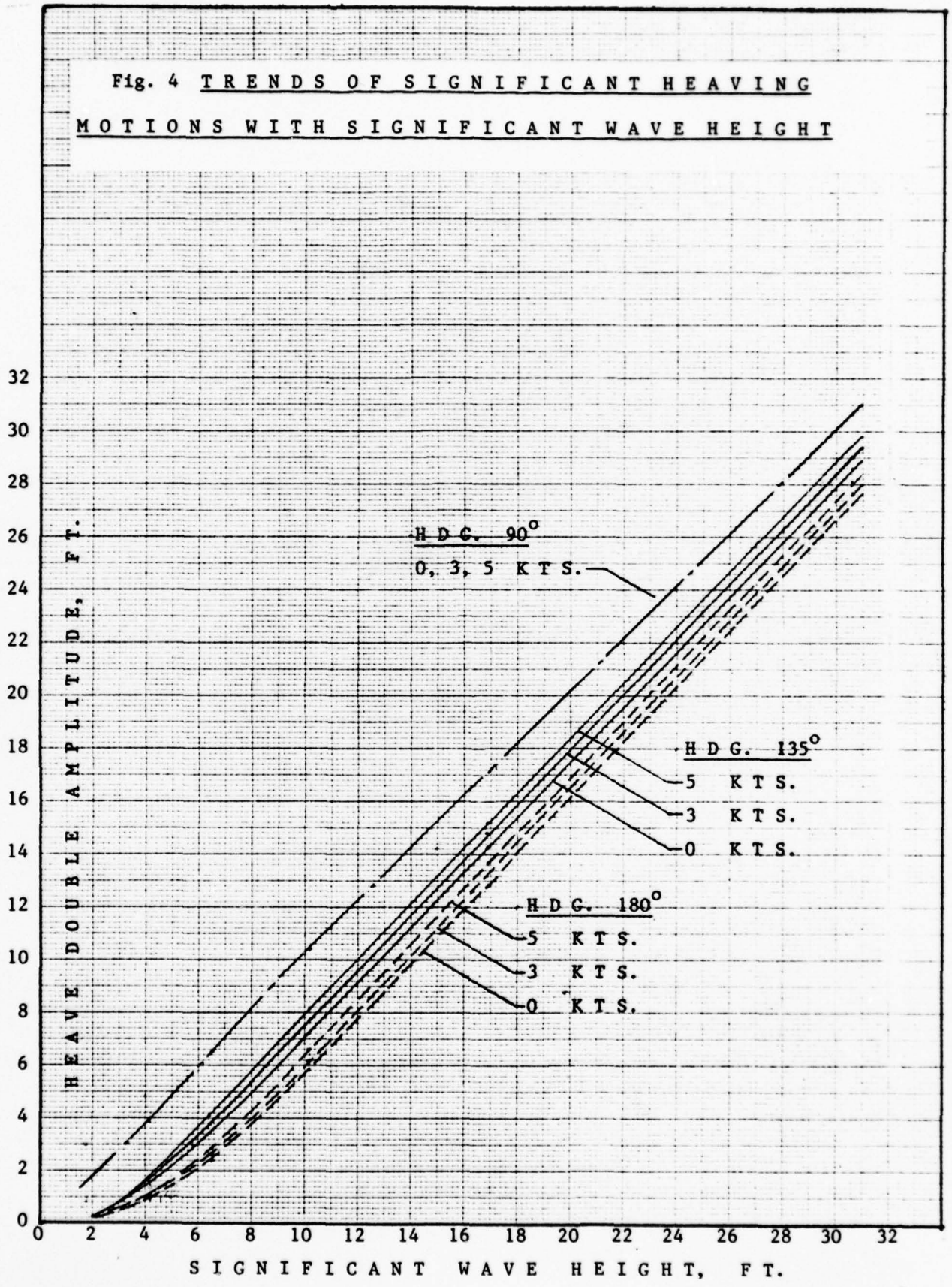

Fig. 5 TRENDS OF SIGNIFICANT PITCHING MOTIONS WITH SIGNIFICANT WAVE HEIGHT

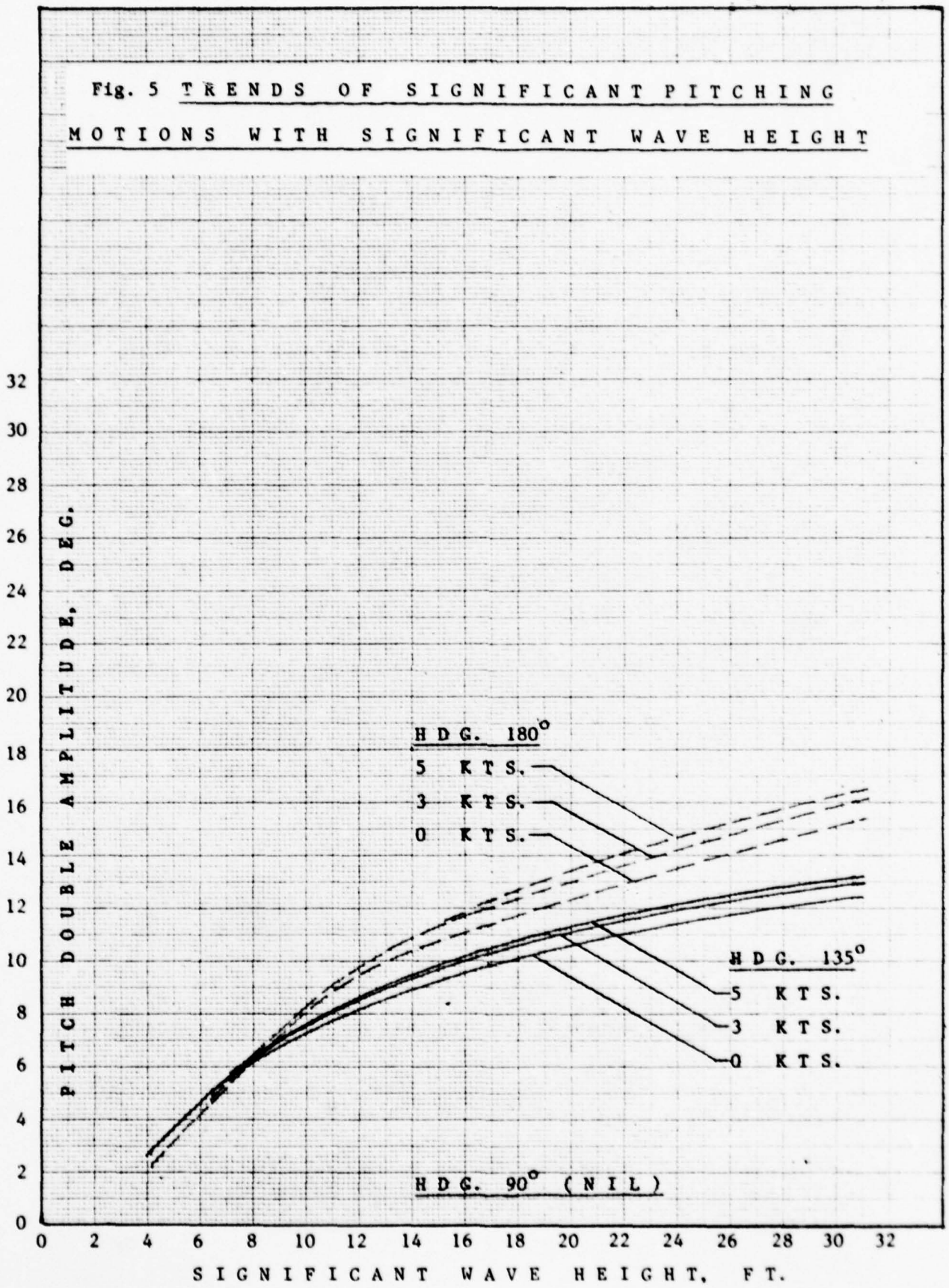

Fig. 6 TRENDS OF SIGNIFICANT ROLLING MOTIONS WITH SIGNIFICANT WAVE HEIGHT

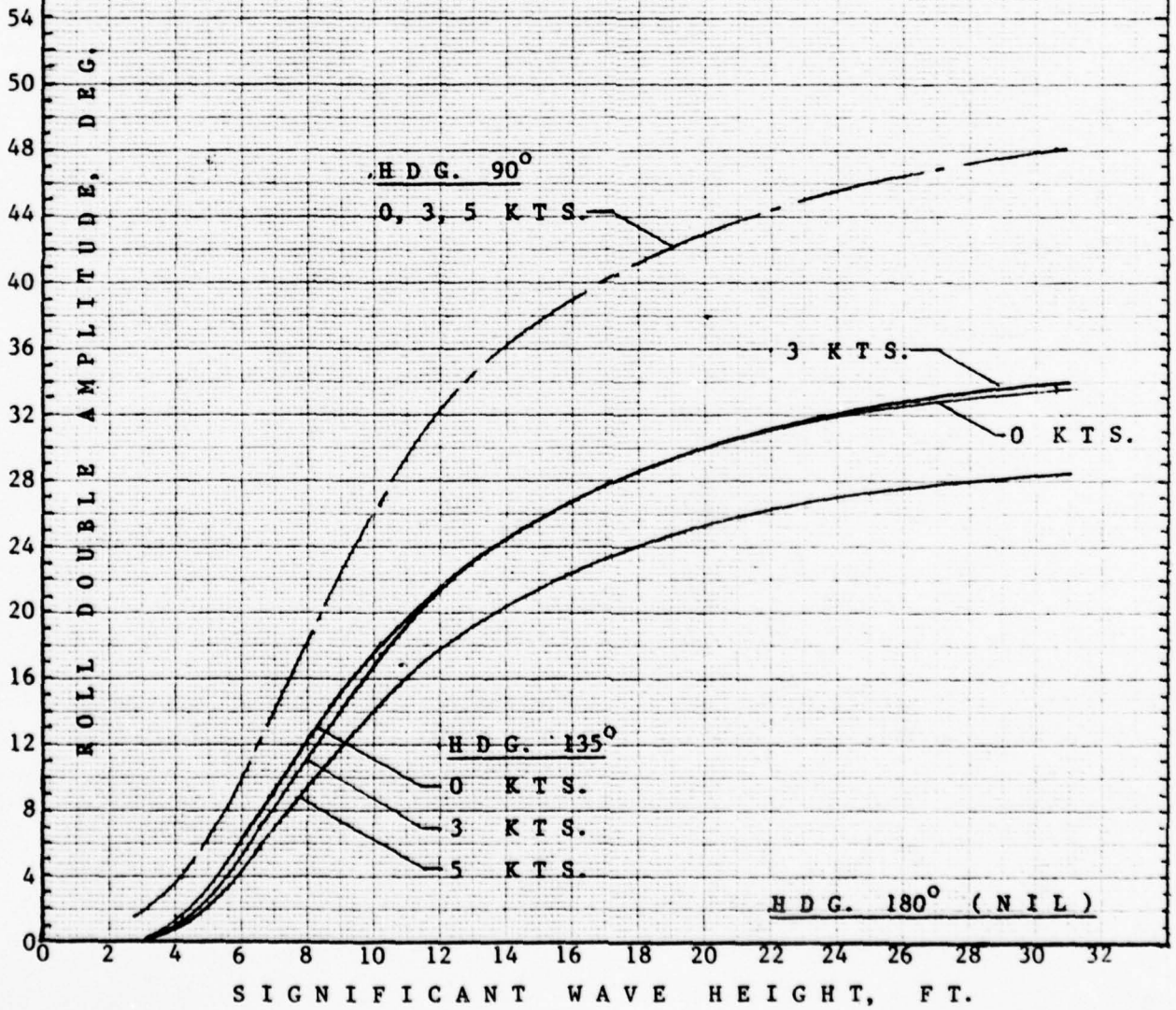

strongly dependent on Significant Wave Height, but only weakly dependent on speed and heading. Weak dependency on speed is also exhibited in the pitching and rolling motions displayed in Figures 5 and 6. The fact that the roll response is flatening out with increasing wave height is due to the relationship of the ship natural roll period to the period of maximum energy in the Seaway Spectrum as discussed above and depicted in Figure 3.

Figures 7, 8, and 9 tell the story of the motions of Points 1, 2, and 3 in the roll mode which as been noted will be the dominant mode. Values for Point 3 only are displayed but values for points 1 and 2 may be inferred by applying the ratios indicated on the figures. As would be expected the trends are similar to those shown in Figure 6. Velocities and accelerations of these points don't really get much worse beyond a State 6, but then State 6 is a severe seaway for a 204-ft. ship. Figure 9 compared to Figure 8 shows that normal accelerations are much smaller than the tangential accelerations.

Figure 10 presents the predictions for vertical motions at the fantail point, Point 4. The amplitudes, velocities and accelerations are all quite moderate and again, show a rather weak dependency on heading and speed.

The foregoing data are tabulated in Table II which gives the ship motion predictions and Table III which gives the point motion predictions. Table III also gives one case of point motion prediction in the pitch mode from which it may be inferred that point motions from this source are modest compared to those

Fig. 7 TRENDS OF ANGULAR AND TANGENTIAL VELOCITY IN ROLL

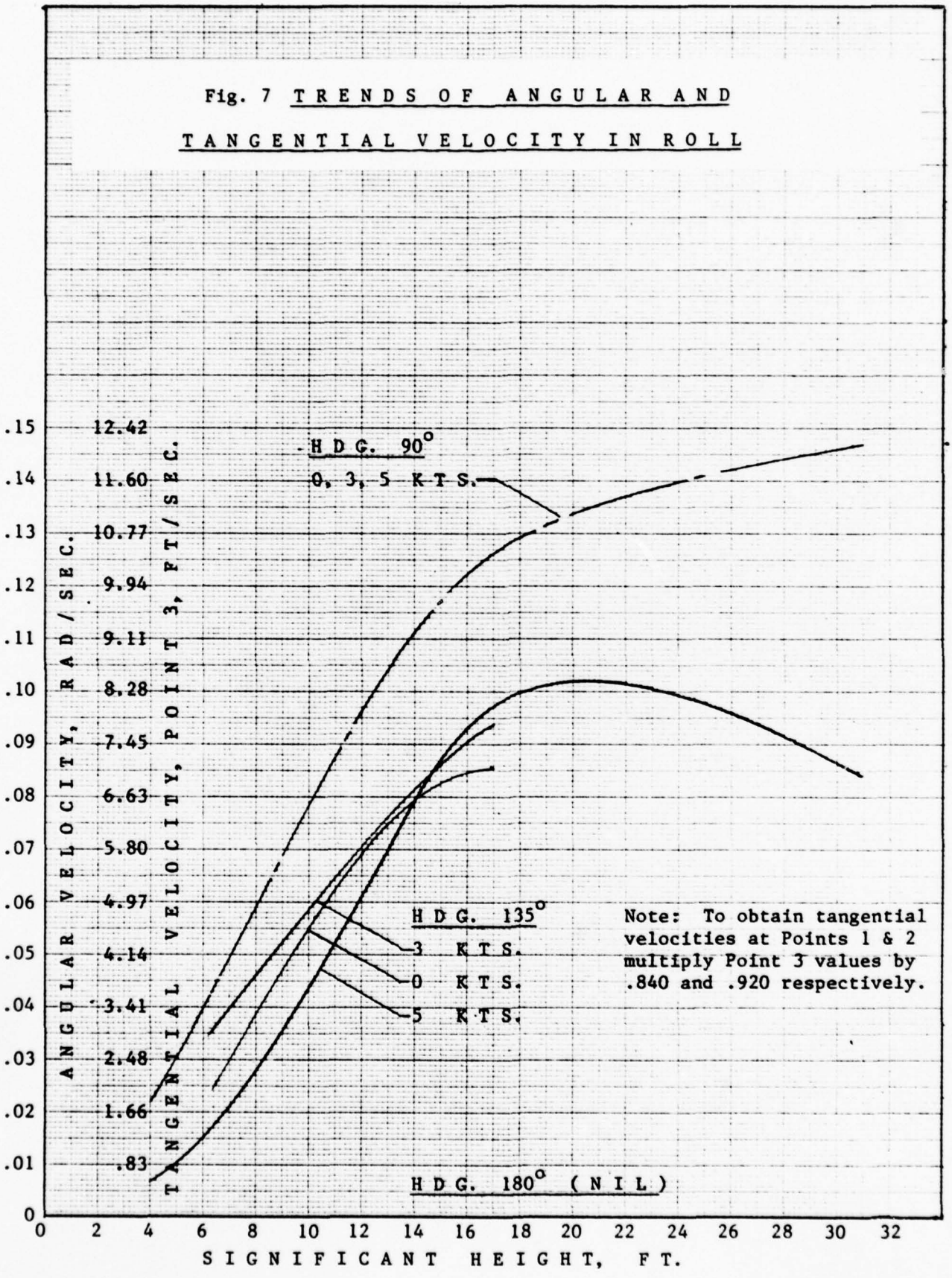

Fig. 8 TRENDS OF ANGULAR AND TANGENTIAL ACCELERATION IN ROLL

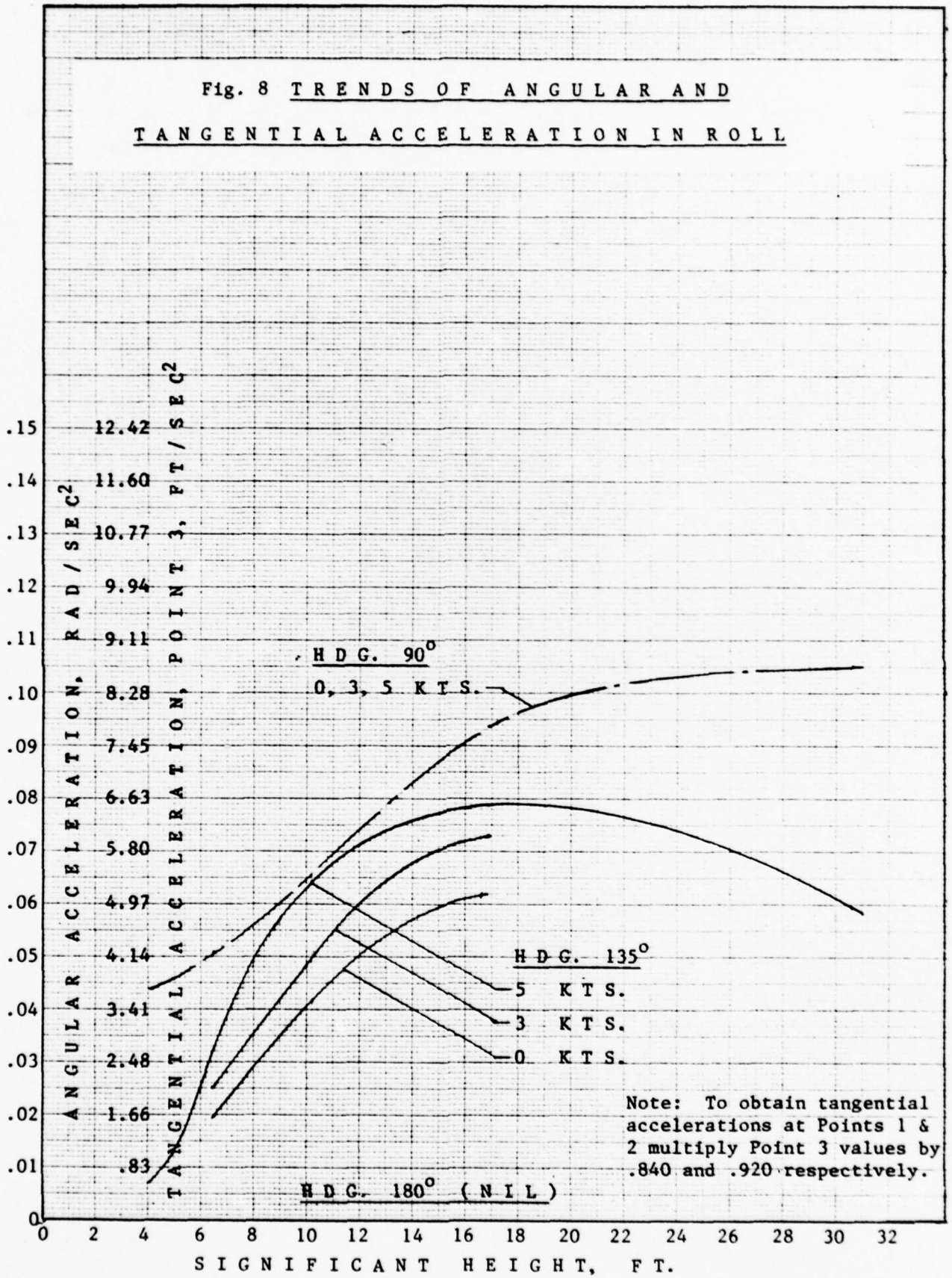

Fig. 9 TRENDS OF NORMAL ACCELERATION IN ROLL

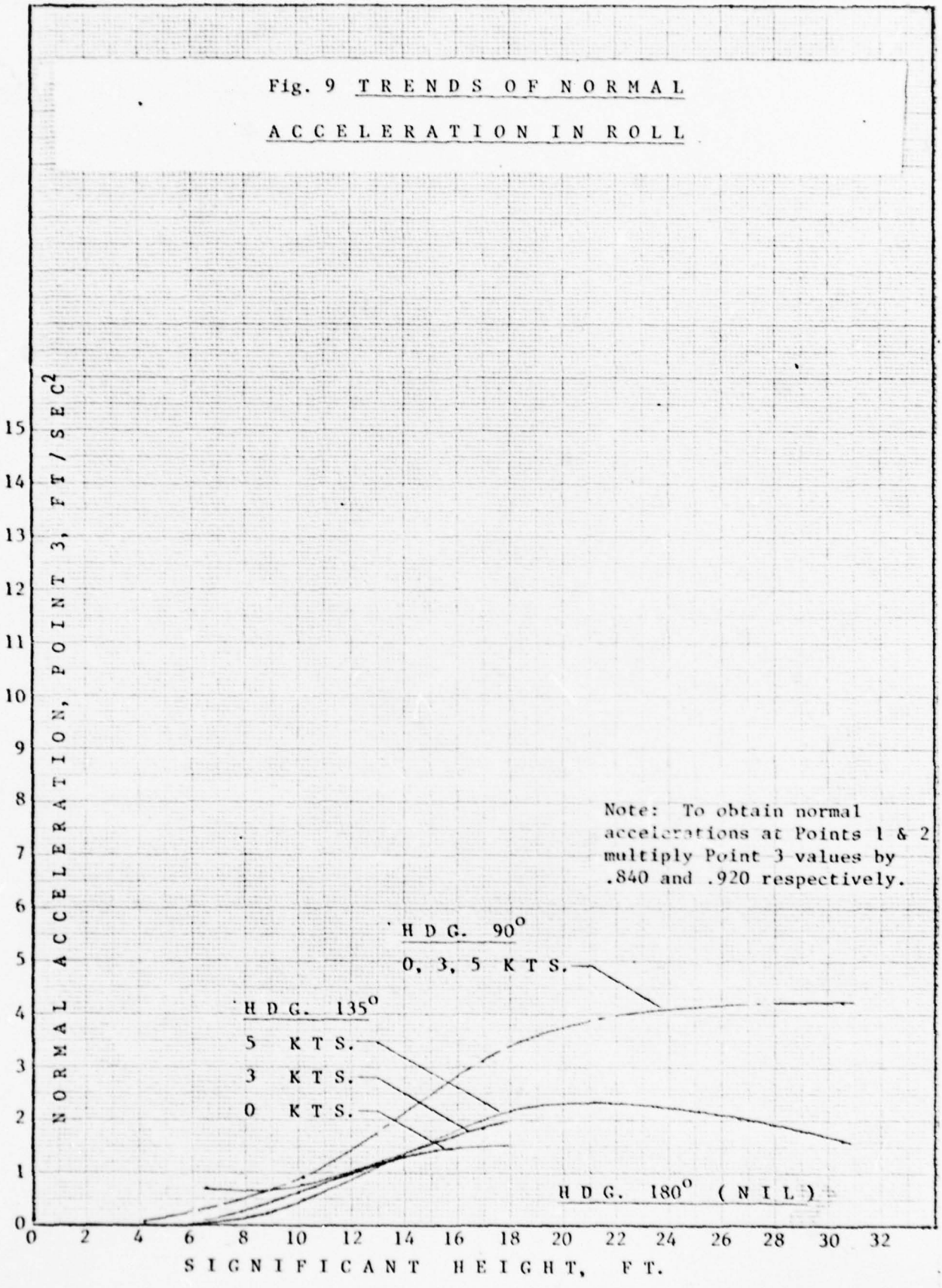

Fig. 10 TRENDS OF VERTICAL MOTIONS AT POINT 4

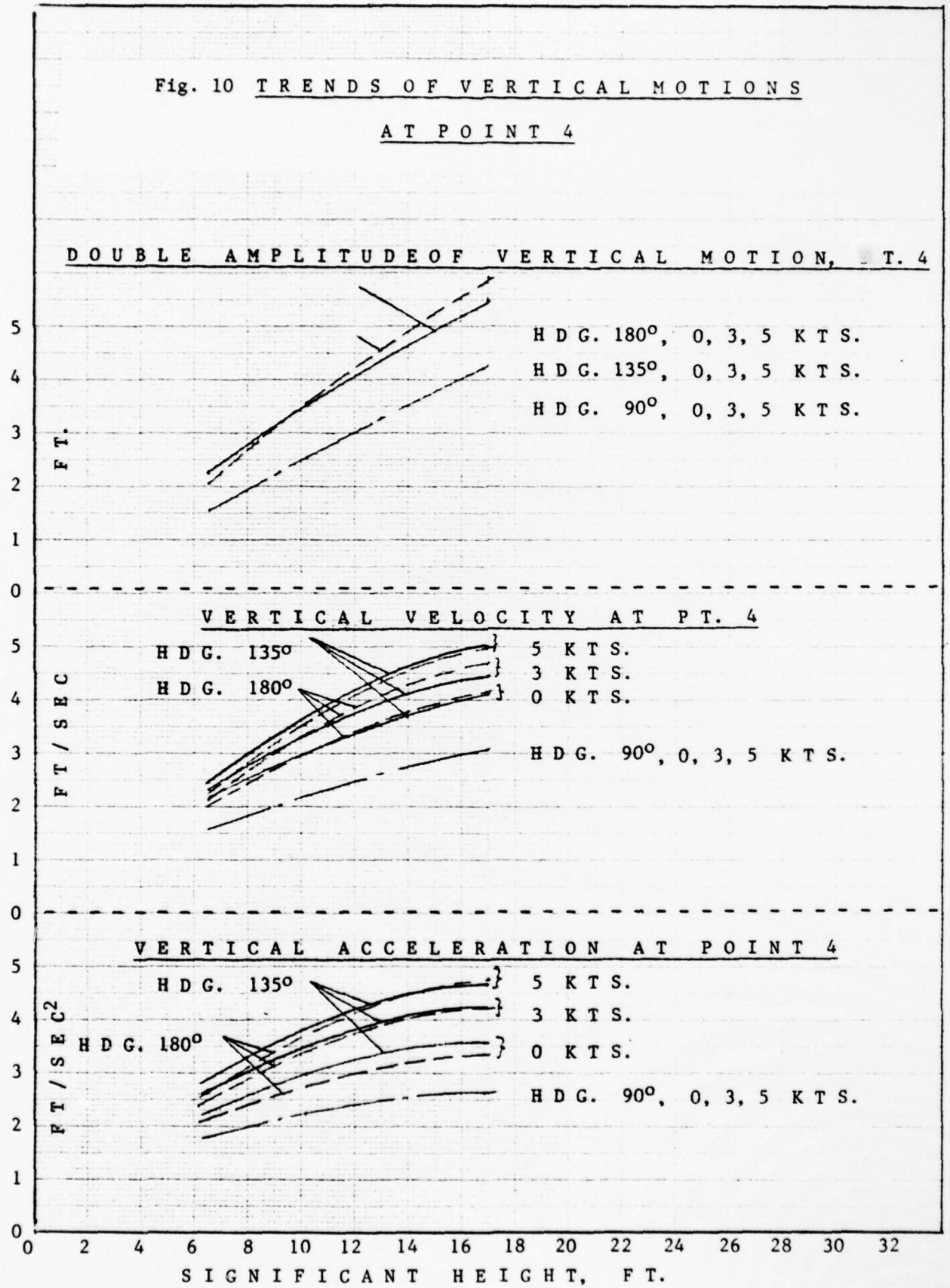

stemming from roll. Transverse accelerations at Point 4 are also included.

It should be borne in mind that all of the above deal with short term predictions, that is motions resulting from a storm condition which may remain stationary for a matter of only a few hours. In the next section we will build on this data base to extend the predictions into the long-term.

TABLE II

RESULTS OF SHORT TERM SHIP MOTION PREDICTIONS[1]
(Average highest motions are given in double amplitudes)

	STATE 4			STATE 5			STATE 6		
Heading Angle[2]	Sig.Ht. = 6.5 ft. 180°	135°	90°	Sig.Ht. = 10.2 ft. 180°	135°	90°	Sig.Ht. = 16.9 ft. 180°	135°	90°
SPEED 0.0 kts.									
HEAVE									
RMS	.59	.86	1.64	1.45	1.81	2.60	3.20	3.58	4.29
Avg.1/3 highest	2.38	3.45	6.56	5.80	7.24	10.43	12.80	14.33	17.16
Avg. 1/10 highest	3.03	4.40	8.37	7.40	9.23	13.30	16.31	18.27	21.88
Avg. 1/1000 highest	4.57	6.64	12.63	11.17	13.94	20.08	24.63	27.58	33.03
PITCH									
RMS	1.2	1.3	.2	1.9	1.8	.2	2.8	2.5	.2
Avg.1/3 highest	4.7	5.0	.7	7.7	7.4	.7	11.3	9.9	.6
Avg.1/10 highest	5.9	6.4	.9	9.8	9.4	.9	14.4	12.6	.8
Avg. 1/1000 highest	9.0	9.7	1.3	14.8	14.2	1.3	21.8	19.0	1.2
SWAY									
RMS	0.	.47	.94	0.	1.00	1.69	0.	2.11	3.25
Avg.1/3 highest	0.	1.87	3.77	0.	3.99	6.78	0.	8.44	12.99
Avg.1/10 highest	0.	2.39	4.80	0.	5.08	8.64	0.	10.76	16.56
Avg.1/1000 highest	0.	3.60	7.25	0.	7.68	13.05	0.	16.24	25.0
ROLL									
RMS	0.	1.9	3.0	0.	4.5	6.6	0.	6.9	10.0
Avg.1/3 highest	0.	7.8	12.1	0.	18.1	26.5	0.	27.6	40.1
Avg.1/10 highest	0.	9.9	15.4	0.	23.0	33.8	0.	35.2	51.1
Avg.1/1000 highest	0.	15.0	23.3	0.	34.8	51.0	0.	53.2	77.1
YAW									
RMS	0.	.5	.1	0.	.8	.2	0.	1.2	.3
Avg.1/3 highest	0.	2.0	.5	0.	3.2	.8	0.	4.6	1.1
Avg.1/10 highest	0.	2.6	.7	0.	4.1	1.1	0.	5.9	1.4
Avg.1/1000 highest	0.	3.9	1.0	0.	6.2	1.6	0.	8.9	2.1

(Continued)

TABLE II
(Continued)

RESULTS OF SHORT TERM SHIP MOTION PREDICTIONS[1]
(Average highest motions are given in double amplitudes)

	STATE 4			STATE 5			STATE 6		
Heading Angle[2]	Sig.Ht. = 6.5 ft. 180°	135°	90°	Sig.Ht. = 10.2 ft. 180°	135°	90°	Sig.Ht. = 16.9 ft. 180°	135°	90°
Speed 3.0 kts.									
HEAVE									
RMS	.65	.95	1.64	1.54	1.92	2.61	3.31	3.70	4.29
Avg.1/3 highest	2.59	3.79	6.56	6.16	7.67	10.43	13.24	14.78	17.15
Avg.1/10 highest	3.30	4.83	8.36	7.86	9.77	13.29	16.88	18.85	21.86
Avg.1/1000 highest	5.0	7.29	12.62	11.87	14.76	20.07	25.48	28.45	33.01
PITCH									
RMS	1.2	1.3	.1	2.1	1.9	.1	3.0	2.6	.1
Avg.1/3 highest	4.9	5.2	.6	8.2	7.6	.6	12.0	10.3	.5
Avg.1/10 highest	6.2	6.6	.7	10.5	9.7	.7	15.3	13.1	.6
Avg.1/1000 highest	9.4	9.9	1.1	15.8	14.7	1.1	23.1	19.8	.9
SWAY									
RMS	0.	.43	.94	0.	.92	1.70	0.	1.95	3.26
Avg.1/3 highest	0.	1.74	3.77	0.	3.68	6.81	0.	7.80	13.02
Avg.1/10 highest	0.	2.21	4.81	0.	4.70	8.69	0.	9.94	16.61
Avg.1/1000 highest	0.	3.34	7.26	0.	7.09	13.12	0.	15.0	25.07
ROLL									
RMS	0.	1.8	3.0	0.	4.4	6.6	0.	6.9	10.0
Avg.1/3 highest	0.	7.1	12.1	0.	17.5	26.5	0.	27.7	40.1
Avg.1/10 highest	0.	9.0	15.4	0.	22.3	33.8	0.	35.3	51.1
Avg.1/1000 highest	0.	13.7	23.3	0.	33.7	51.0	0.	53.3	77.1
YAW									
RMS	0.	.4	.1	0.	.7	.2	0.	1.0	.3
Avg.1/3 highest	0.	1.8	.5	0.	2.8	.8	0.	4.1	1.1
Avg.1/10 highest	0.	2.2	.7	0.	3.6	1.0	0.	5.2	1.4
Avg.1/1000 highest	0.	3.4	1.0	0.	5.5	1.6	0.	7.9	2.0

(Continued)

TABLE II
(Continued)

RESULTS OF SHORT TERM SHIP MOTION PREDICTIONS[1]
(Average highest motions are given in double amplitudes)

	STATE 4			STATE 5			STATE 6		
Heading Angle[2]	Sig.Ht. = 6.5 ft. 180°	135°	90°	Sig.Ht. = 10.2 ft. 180°	135°	90°	Sig.Ht. = 16.9 ft. 180°	135°	90°
				Speed 5.0 kts.					
HEAVE									
RMS	.72	1.03	1.63	1.64	2.02	2.60	3.42	3.80	4.28
Avg.1/3 highest	2.87	4.13	6.52	6.57	8.08	10.39	13.68	15.20	17.13
Avg.1/10 highest	3.66	5.26	8.31	8.38	10.30	13.25	17.44	19.38	21.84
Avg.1/1000 highest	5.52	7.95	12.55	12.65	15.56	20.0	26.34	29.26	32.98
PITCH									
RMS	1.2	1.3	.1	2.1	1.9	.1	3.1	2.6	.1
Avg.1/3 highest	4.9	5.1	.5	8.4	7.7	.5	12.3	10.4	.4
Avg.1/10 highest	6.3	6.5	.6	10.8	9.8	.6	15.7	13.3	.5
Avg.1/1000 highest	9.5	9.9	1.0	16.3	14.9	1.0	23.8	20.1	.8
SWAY									
RMS	0.	.41	.95	0.	.88	1.71	0.	1.85	3.26
Avg.1/3 highest	0.	1.65	3.78	0.	3.51	6.84	0.	7.41	13.04
Avg.1/10 highest	0.	2.10	4.82	0.	4.47	8.72	0.	9.45	16.63
Avg.1/1000 highest	0.	3.18	7.28	0.	6.75	13.16	0.	14.27	25.10
ROLL									
RMS	0.	1.5	3.0	0.	3.6	6.6	0.	5.8	10.0
Avg.1/3 highest	0.	5.9	12.1	0.	14.3	26.5	0.	23.0	40.1
Avg.1/10 highest	0.	7.5	15.4	0.	18.2	33.8	0.	29.4	51.1
Avg.1/1000 highest	0.	11.3	23.3	0.	27.5	51.0	0.	44.3	77.1
YAW									
RMS	0.	.4	.1	0.	.7	.2	0.	1.0	.3
Avg.1/3 highest	0.	1.6	.6	0.	2.7	.9	0.	3.8	1.3
Avg.1/10 highest	0.	2.1	.7	0.	3.4	1.2	0.	4.9	1.6
Avg.1/1000 highest	0.	3.1	1.1	0.	5.1	1.8	0.	7.3	2.5

[1]Using experimentally generated roll RAO's
[2]Angle between direction of ship and direction of waves.
180° = head seas, 135° = bow seas, 90° = beam seas.

TABLE III

RESULTS OF SHORT TERM POINT MOTION PREDICTIONS[1]
(RMS of maximum values)

	STATE 4			STATE 5			STATE 6		
Heading Angle[2]	Sig.Ht. = 6.5 ft. 180°	135°	90°	Sig.Ht. = 10.2 ft. 180°	135°	90°	Sig.Ht. = 16.9 ft. 180°	135°	90°
POINT 3[3], SPEED 0 kts.									
ROLL									
Ang.Vel.rad/sec	0.	0.0253	0.0450	0.	0.0560	0.0745	0.	0.0857	0.1259
Ang.Accel.rad/sec^2	0.	0.0194	0.0505	0.	0.0415	0.0655	0.	0.0615	0.0935
Tang.Vel.ft/sec	0.	2.10	3.72	0.	4.69	6.17	0.	7.10	10.42
Tang.Accel.ft/sec^2	0.	1.61	4.18	0.	3.44	5.43	0.	5.09	7.75
Norm.Accel.ft/sec^2	0.	0.124	0.27	0.	0.663	0.90	0.	1.51	3.09
POINT 3, SPEED 3 kts.									
ROLL									
Ang.Vel.rad/sec	0.	0.0365	0.0450	0.	0.0600	0.0745	0.	0.0932	0.1259
Ang.Accel.rad/sec^2	0.	0.0250	0.0505	0.	0.0480	0.0655	0.	0.0730	0.0935
Tang.Vel.ft/sec	0.	3.02	3.72	0.	4.97	6.17	0.	7.72	10.42
Tang.Accel.ft/sec^2	0.	2.07	4.18	0.	3.98	5.43	0.	6.05	7.75
Norm.Accel.ft/sec^2	0.	0.721	0.27	0.	0.770	0.90	0.	1.86	3.09
POINT 3, SPEED 5 kts.									
PITCH									
Ang.Vel.rad/sec							0.0419		
Ang.Accel.rad/sec^2							0.0350		
Tang.Vel.ft/sec^2							3.47		
Tang.Accel.ft/sec^2							2.90		
Norm.Accel.ft/sec^2							.1988		
ROLL									
Ang.Vel.rad/sec	0.	0.0182	0.0450	0.	0.0453	0.0745	0.	0.0969	0.1259
Ang.Accel.rad/sec^2	0/	0.0322	0.0505	0.	0.0640	0.0655	0.	0.0785	0.0935
Tang.Vel.ft/sec	0.	1.35	3.72	0.	3.75	6.17	0.	8.03	10.42
Tang.Accel.ft/sec^2	0.	2.45	4.18	0.	5.30	5.43	0.	6.51	7.75
Norm.Accel.ft/sec^2	0.	0.02	0.27	0.	0.48	0.90	0.	1.96	3.09

(Continued)

TABLE III
(Continued)

RESULTS OF SHORT TERM POINT MOTION PREDICTIONS[1]
(RMS of maximum values)

	STATE 4			STATE 5			STATE 6		
Heading Angle[2]	Sig.Ht. = 6.5ft.			Sig.Ht = 10.2 ft.			Sig.Ht. = 16.9 ft.		
	180°	135°	90°	180°	135°	90°	180°	135°	90°
POINT 4, SPEED 0 kts.									
VERTICAL MOTION									
Dbl.Amplitude, ft.	2.06	2.23	1.52	3.58	3.54	2.52	5.78	5.46	4.24
Velocity, ft/sec	1.96	2.19	1.58	2.98	3.11	2.21	4.14	4.11	3.03
Accel., ft/sec^2	2.05	2.27	1.85	2.72	2.96	2.25	3.33	3.53	2.59
TRANSVERSE ACCELERATION									
Trans.Accel.ft/sec^2	0.	1.16	1.72	0.	1.49	2.20	0.	1.71	2.52
POINT 4, SPEED 3 kts.									
VERTICAL MOTION									
Dbl.Amplitude, ft.	2.04	2.19	1.56	3.63	3.55	2.55	5.88	5.50	4.26
Velocity, ft/sec	2.12	2.35	1.58	3.35	3.38	2.22	4.68	4.47	3.06
Accel. ft/sec^2	2.38	2.66	1.80	3.35	3.50	2.23	4.20	4.20	2.61
TRANSVERSE ACCELERATION									
Trans.Accel.ft/sec^2	0.	1.26	1.68	0.	1.66	2.18	0.	1.95	2.52
POINT 4, SPEED 5 kts.									
VERTICAL MOTION									
Dbl.Amplitude, ft.	2.00	2.15	1.59	3.63	3.53	2.57	5.91	5.52	4.28
Velocity, ft/sec	2.21	2.43	1.60	3.56	3.52	2.25	5.00	4.69	3.08
Accel., ft/sec^2	2.61	2.89	1.78	3.78	3.85	2.23	4.78	4.63	2.63
TRANSVERSE ACCELERATION									
Trans.Accel.ft/sec^2	0.0	1.30	1.65	0.0	1.76	2.17	0.0	2.09	2.53

[1]Using experimentally generated roll RAO's.
[2]Angle between direction of ship and direction of waves.
180° = head seas, 135° = bow seas, 90° = beam seas.
[3]To obtain values for Points 1 and 2 multiply Point 3 values cited by the ratio of their vertical distances to the center of gravity, that is, multiply by .840 and by .920 respectively.

4.0 Design Criteria Development

The objective of this section is to develop a set of curves to be used by the ship designer in establishing the limits of linear and angular motions (displacements, velocities and accelerations) based on desired probabilities of exceedance or frequencies of occurrence over a period of ship operating time.

4.1 Current State-of-the-art

For several years the process of predicting wave-induced loads for design purposes has consisted of the following steps and assumptions.

1. It is usually assumed that ocean waves can be represented by "Pierson-Moskowitz" spectra, and that this spectral form could be considered sufficiently "narrow" to allow a Rayleigh distribution to be used to predict the amplitudes of the peaks and troughs. Several workers (Reference 3, for example) have recently expressed doubts as to the validity of these assumptions, particularly with reference to the extreme conditions that must generate design loads. The Pierson-Moskowitz spectra were intended to represent fully developed sea waves (Reference 4). Fully-developed seas are only generated if the wind blows for a long enough duration over an extensive enough fetch. The requirements for both duration and fetch become larger as the

wind speed increases and, for severe storms, become quite unrealistic as shown in Table IV and Figure 11, so anything approaching a "fully-developed" extreme sea state is extremely improbable. For example, Figure 11 shows that above Sea State 7 the storm duration required for a fully arisen sea exceeds the total time expected for that sea state in one year. The theoretically attainable wave heights also shown in Figure 11 will almost certainly not be reached in the higher sea states for the same reason, so that the highest waves and consequently, the highest wave-induced loads may actually occur in lower sea states due to their greater duration. In a similar way the Rayleigh distribution function is very adequate to describe light to moderate sea states but does not describe severe sea states with much realism. The fact that the highest loads are to be expected in the more frequently occurring medium sea states rather than in the rare extreme sea states was pointed out in Reference 6, based on full-scale experimental evidence. There has recently been a tendency at NSRDC to propose that calculations of extreme loads should be made from measured extreme wave spectra but this method is inconsistent with the evidence referred to above.

2. The second major assumption is that of linear response. Clearly if responses such as heave, pitch, bending-moment, vertical acceleration, etc. can be considered to be linear with respect to the wave then the process of calculating extreme motions becomes

Table IV Standard Sea State Parameters (Reference 5)

SS	0	1	2	3	4	5	6	7	8	9
$h_{1/3}$ (ft)	.18	1.2	3.1	5.3	7.4	12.5	20	42	61	">128"
Wind Speed (Kn)	3.5	9	13.5	17	19.5	24	29	39	45	>64
Average Period, $\overline{T}$ (secs)	1.4	2.6	3.9	4.8	5.5	6.9	8.2	11.0	12.8	>18
Percentage of Time (N. Atlantic)	17%			28%	25%	21.5%	6.5%	1.97%	.0293%	.0007%
Time in One Year (hrs.)	1489			2453	2190	1883	569	173	26	3.7 Min.
Number of Waves/Yr. (millions)				2.1	1.5	1.1	.27	.065	.0079	14×10^{-6}
Average Highest Expected Wave (ft)	3.2			11.3	16.8	26.13	40.8	73.0	108	107
Conditions for "fully developed sea" (1)										
Duration (hr)	2.2		5.0	7.0	9.5	14	21.5	40	103	490
Fetch (n.m.)	9		27	47	70	130	255	655	2700	30,000

(1) Pierson, W. J., Neumann, G., and James, R. W., OBSERVING AND FORECASTING WAVES, H. O. Pub. No. 603, U. S. Naval Oceanographic Office (1971)

Fig. 11 Characteristics of Ocean Waves.
(ref. 5)

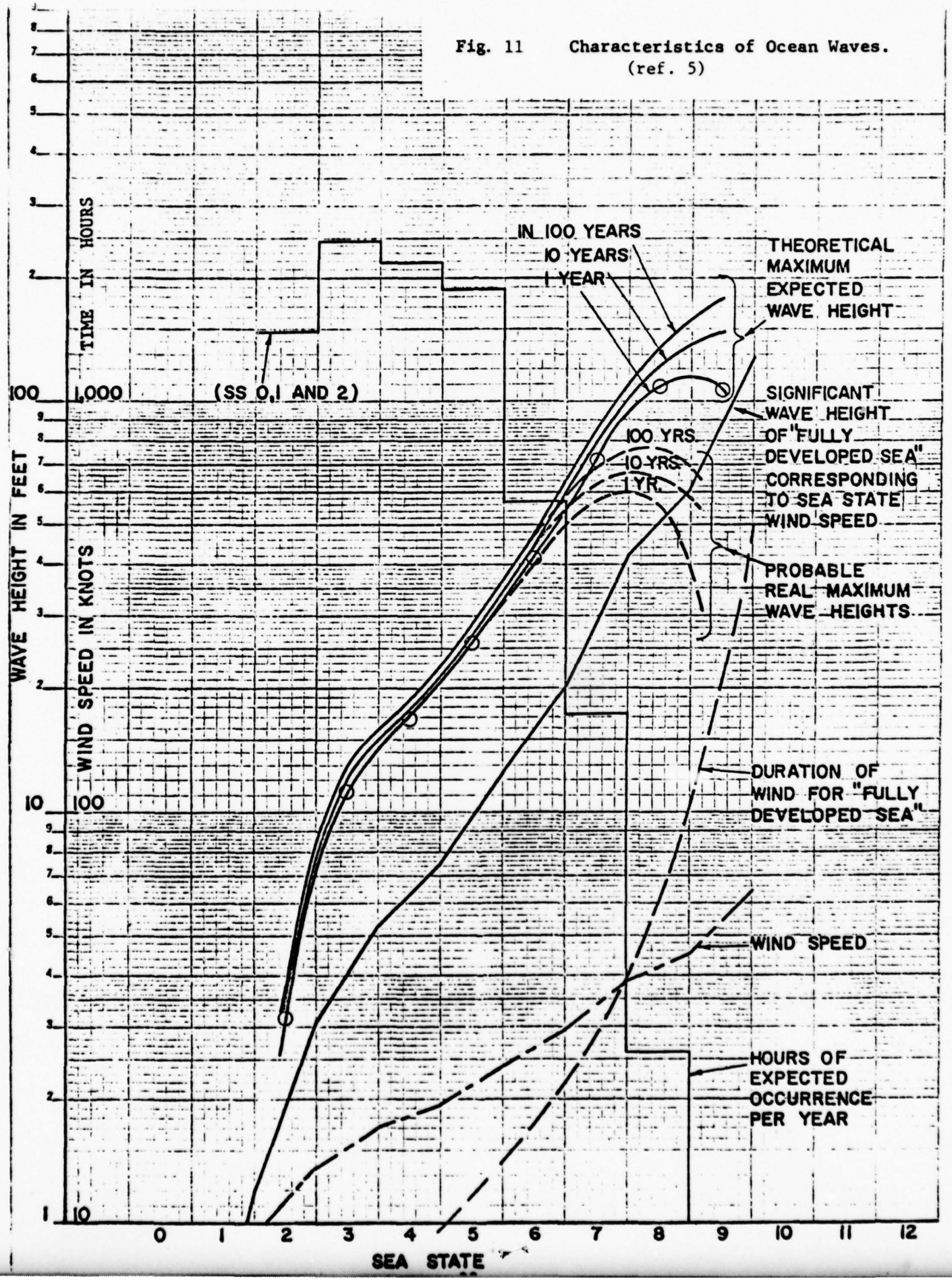

rather simple. This is a very real consideration and many authorities, notably E. V. Lewis, for example, in Reference 7, maintain that it is preferable to use a manageable design technique that is known to be somewhat approximate rather than a more exact analysis that is too complex to apply in practice at this time. Largely for this reason the linear response theory has been adhered to long after it has clearly and repeatedly been proven not to apply to high performance marine vehicles. One reason for this has been that, for conventional ships, References 6, 7, 8, 9 and many others have shown that the linear assumption gives very acceptable agreement with full-scale and model tank measurements. For planing craft, surface effect ships, etc., the craft geometry and the dynamic forces acting on the hull vary in a markedly nonlinear fashion. For the case of roll motion which is a highly nonlinear mode and, more specifically for rolling motions of a hard chine hull such as that of the T-AGOS, the assumption of linearity no longer holds and a different course of action must be followed in to order to predict the long term extremes for design purposes. For example, Figure 12 shows typical peak vertical acceleration distribution for the SES-100B testcraft in Sea State 3. The distribution used here to approximate the data is the Weibull distribution (to be discussed later) of which the Rayleigh and Exponential distributions are special cases (all that changes is the gradient of the curve). In the case of Figure 12 the Weibull distribution which fits the data has a

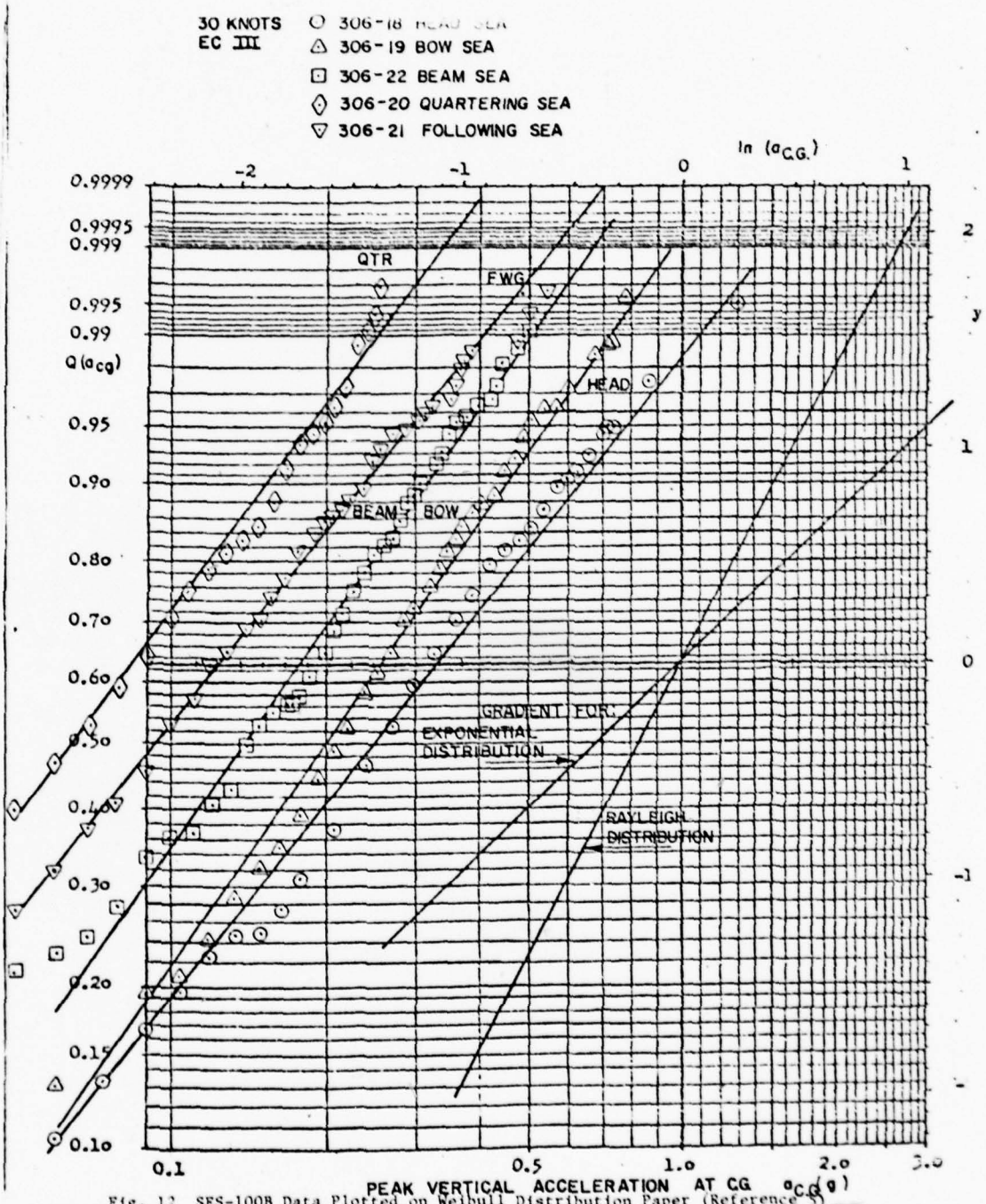

Fig. 12 SES-100B Data Plotted on Weibull Distribution Paper (Reference 5)

gradient which falls between that of the Rayleigh and Exponential as is clearly demonstrated. Thus for this particular case one would use a distribution with the best fitting gradient to predict the long-term extreme motions and loads given a certain acceptable probability or frequency of occurrence established apriori.

On the basis of these observations it is hypothesized that the Weibull distribution may be said to represent long term roll data in a reasonable manner, and is a clear improvement on either the exponential or the Rayleigh distributions which are, in turn, one-parameter special cases of the Weibull distribution. The Weibull distribution is also acceptable from the point of view that it is closely related to the Rayleigh distribution which is the generally accepted representation of wave-heights and wave-induced phenomena.

In order to make use of the Weibull distribution in the analysis of extreme values some of its characteristics must be understood. These are presented in Appendix (I).

4.2 Prediction of long-term extreme values

The rms values predicted by the MIT 5-DOF program can now be used in conjunction with the Weibull distribution in order to predict the long term extreme values of motions, including displacements, velocities and accelerations. Having obtained these long

term distribution curves then the design criteria can be applied in order to obtain the desired limit motions and their frequency of occurrence from the curves.

As discussed in Appendix (I) the Weibull distribution probability density function is given by:

$$f(x) = c\lambda^c \, x^{c-1} \exp\{-(\lambda x)^c\} \qquad (1)$$

The value of λ can be defined in terms of the r.m.s. value r and the Gamma function Γ:

$$\frac{1}{\lambda} = \frac{r}{\{\Gamma(1+2/c)\}^{\frac{1}{2}}} \equiv \frac{r}{\Gamma} \qquad (2)$$

The cumulative probability can be expressed as:

$$P(x_j) = \exp\{-(\lambda x)^c\} \qquad (3)$$

or in terms of r:

$$P(x_j) = \exp\{-(\frac{x\Gamma}{r})^c\} \qquad (4)$$

$P(x_j)$ is the probability of exceeding a value x_j which in our specific case are amplitudes of displacement, velocity and acceleration. The exponent c is a constant which represents the gradient of the distribution curve. Clearly equation (4) tells us that depending on the value of the exponent c, the degree of conservativism in the prediction of the long-term extremes will vary.

The effect of the choice of distribution on the long term motions may be seen most graphically in Figure I.4 of Appendix (I). At the higher levels of probability, which are those of interest in establishing extreme values, the long-term cumulative

distribution curves fan out over a wide range for different values of the parameter c. This difference may be reduced somewhat if it is hypothesized that these distributions should not be compared with respect to the rather abstract parameter x, but should rather be compared on the basis of the ratio x/r of x to the rms value. The variation of r with variation of the parameter c is shown in Figures I.1 and I.2 of Appendix (I). Figure 13, therefore, shows the long term distributions of x/r for various c values.

Now each run in a test tank, of the full-scale vessel or a computer run with the motions program is necessarily a short-term event. During each short-term event, it is assumed that each ship's speed and heading and the sea state remain constant. The operational life of a ship can be considered as a summation of a very large number of short term events. If the behavior in each short-term event is known, and also if the manner of distribution of short-term events throughout the ship's life is known, then a long-term picture of the ship's life can be built up. This is the method used here to predict the long-term behavior of the vehicle so that eventually, a single long-term distribution of motions (or loads or stresses) can be built up to represent the ship's total experience in all speeds, sea states, headings and loading conditions. In order to accomplish this, use is made of the description of the operational environment as shown in figure (11) as well as the operating envelope (forward speed vs sea state).

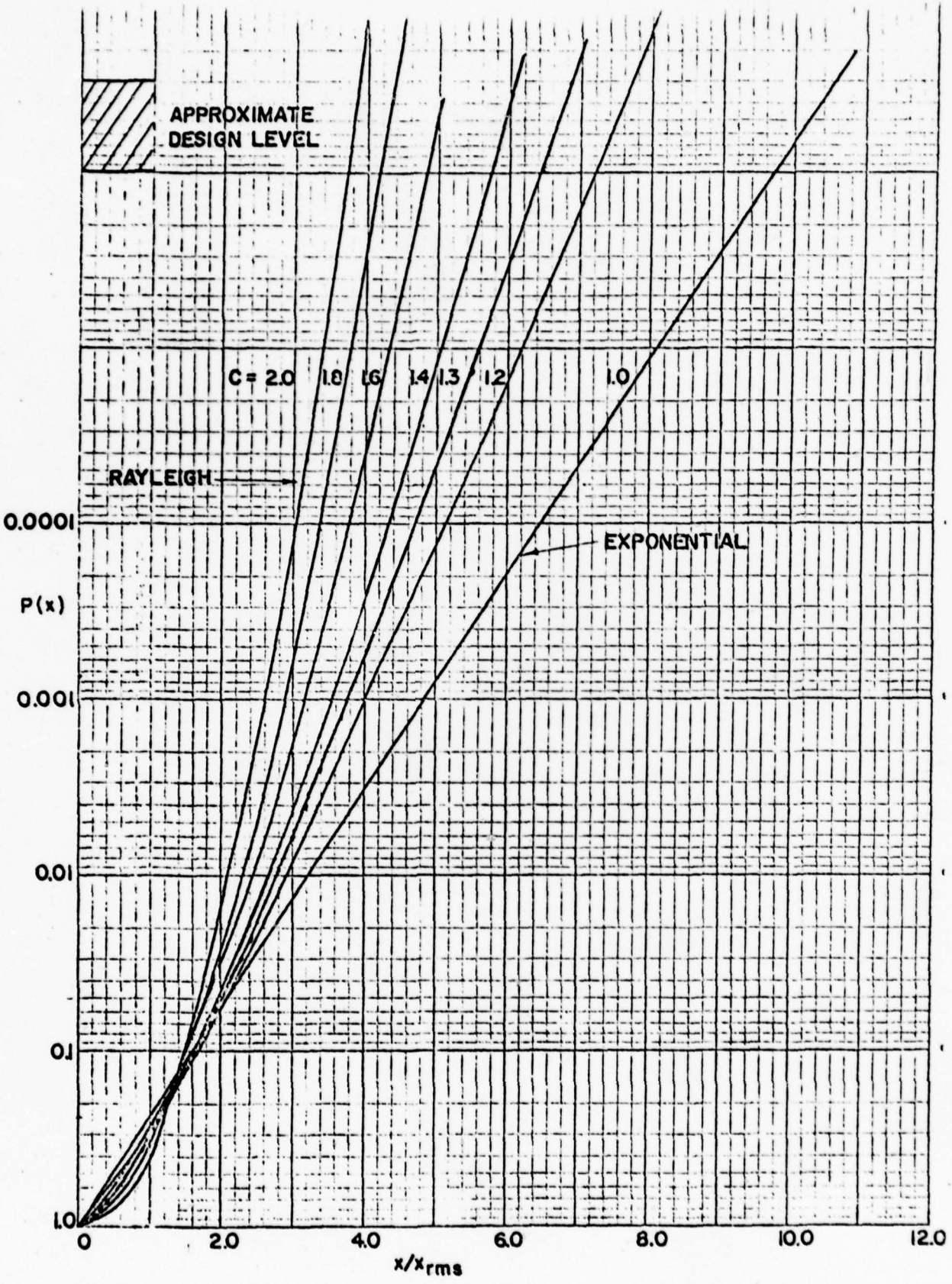

Fig. 13 Weibull Cumulative Distribution of x/x_{rms}. (ref. 5)

If the probability of exceeding a given motion x at a speed V, in sea state S, at heading H and displacement W, is $P_{VHSW}(x)$, then the total probability P(x) of exceeding the motion x is given by summing the component probabilities for all conditions

$$P(x) = \sum_{V}\sum_{H}\sum_{S}\sum_{W} P_V \cdot P_H \cdot P_S \cdot P_W \cdot P_{VHSW}(x) \qquad (5)$$

where P_V, P_H, P_S, P_W are the probabilities of occurrence of each velocity, heading, sea state and displacement respectively.

For the purposes of this effort however, a few simplifications will have to be made since no information has been provided on the operating envelope and the displacement probabilities of the T-AGOS. Thus the combined probability of exceeding a motion level x is taken here as

$$P(x) = \sum_{S} P_S \cdot P_S(x) \qquad (6)$$

where P_V, P_W, and P_H are not taken into consideration. Instead, P(x) is computed using equation (6) for specified displacement, heading and speed. However, as the information on the operating envelope is made available, then a more rigorous calculation could be conducted. The use of equation (6) will yield a conservative estimate since P_V, P_H, and P_W are not considered.

5.0 Design Criteria Recommendations

A reasonable criteria for selecting the design motion level for the T-AGOS is to select that displacement, velocity or

acceleration which would occur once in a certain period of operation. For example, based on a nominal 2000 hours per year at sea, the frequency of occurrence F, of once in 2000 hours can be expressed as

$$T = 2000 \text{ hours} \times 3600 \frac{\text{seconds}}{\text{hour}}$$

$$= 7.2 \times 10^{6} \text{ secs}$$

$$F = 1/T = \frac{1}{7.2 \times 10^{6}} = 0.139 \times 10^{-6} (\text{sec}^{-1})$$

Now for any single short-term distribution of the frequency of occurrence F(x) of any parameter x is given by

$$F(x) = nP(x) \tag{7}$$

where n is the number of occurrences per unit time and P(x) is the probability of exceeding x in any one excursion. Both f(x) and n have dimensions of, for example, (sec^{-1}). Thus the combined frequency F(x) of exceeding any particular level, x, of motion response is obtained from equations (6) and (7) and is given by

$$F(x) = nP(x) = \sum_{S} n \, P_S \cdot P_S(x) \tag{8}$$

The parameter n is a function of displacement, speed, sea state and heading.

The average period of rolling is

$$T_{\eta_4} = \frac{2\pi\eta_4}{\dot{\eta}_4} \tag{9}$$

where η_4 = rms roll amplitude

$\dot{\eta}_4$ = rms roll velocity

The number of occurrences, n, per unit time is then given by

$$n = \frac{1}{T_{\eta_4}} = \frac{\dot{\eta}_4}{2\pi\eta_4} \tag{10}$$

where η_4 and $\dot{\eta}_4$ are the rms values for given sea state, heading, displacement and speed.

The value of n given by (10) is then substituted in (8) in order to obtain the combined frequency of occurrence F(x).

For our purposes we will consider the beam seas roll case as being the most critical. This is indicated by the output of the computer simulations where the largest rms amplitudes of roll occurred in beam seas and increased with increasing sea state. For the beam sea condition forward speed (0, 3, 6 knots) had no effect on roll.

Table (V) summarizes the data needed to develop long term distribution curves for each of the six parameters of interest, i.e., η_4, $\dot{\eta}_4$, $\ddot{\eta}_4$, V_t, a_t, and a_n. In addition to the rms values of these variables as a function of sea state for beam seas and forward speeds of 0, 3, and 6 knots, Table (V) also shows the probability of occurrence of each sea state, P_s, which has been

TABLE V Roll motions as a function of Sea State ($\gamma = 90^{o}$; V = 0, 3, 5 knots; R = 82.83')

Sea State, $\bar{H}_{1/3}$(ft)	η_4	$\dot{\eta}_4$	$\ddot{\eta}_4$	V_t	a_t	a_n	T_{η_4}	n	P_s
S.S.3	(radians)	(rad/sec)	(rad/sec^2)	(ft/sec)	(ft/sec^2)	(ft/sec^2)	(sec)	(sec^{-1})	
4.2	.0171	.0238	.0439	1.97	3.64	.03	4.51	.222	.28
S.S.4									
6.5	.0527	.0450	.0505	3.72	4.18	.27	7.35	.136	.25
S.S.5									
10.2	.1002	.0745	.0655	6.17	5.43	.90	8.54	.118	.215
S.S.6									
16.9	.1755	.1259	.0935	10.42	7.775	3.09	8.75	.114	.065
S.S.7									
30.6	.2097	.1467	.1051	12.15	8.17	4.21	8.98	.111	.0197

calculated from figure 11. Likewise the value of n and T are given for each sea state. In all cases the value of R (the distance from the c.g to the point in question) is taken to be the maximum of 82.83 ft.

Since at the present time there is no experimental data (model or full-scale) which would allow one to determine the value of the constant c in the Weibull distribution, it was felt that a reasonable path to follow here was to present long term distribution curves for the six parameters of interest using values of c of 1.3 and 2.0. With c = 1.3 the design levels would be more conservative than in the case of c = 2.0 which corresponds to the Rayleigh distribution. This is clearly illustrated in figure (13). For example, the probability of exceeding the ratio $x/x_{rms} = 3.0$ is .00001 when c = 2.0 while the same ratio is exceeded with a probability of .006 when c = 1.3. In this effort the value of c = 1.3 has been chosen based on observations and analyses of other non-linear phenomena (refs. 5, 10, 11, 12).

Figures (14) through (19) show the results of this procedure for all six variables. In each case design values have been obtained applying the criteria of one exceedance per 2000 hours. Conservative and less conservative estimates are presented depending on the choice of distribution. The former corresponds to a Weibull distribution with parameter c = 1.3 while the latter is a Weibull distribution with c = 2.0 (i.e. the Rayleigh distribution). It is pointed out that these estimates already have a

built-in conservativism due to the assumption of 2000 hours of operation in beam seas which is not operationally realistic. To avoid this situation one must include the probability of heading occurrence in the computation of the total combined probability or frequency of exceedance according to equation (5). However, the curves of figures (14) through (19) do take into account the expected frequency of occurrence of all sea states.

In view of the above assumptions, and the limitations caused by not having an operational envelope defined prior to conducting this study, the long-term design values presented here should be used with caution until a more complete analysis is conducted. As indicated earlier there is no long-term experimental roll data for the T-AGOS or similar hulls. *Until such information becomes available* a value of $c = 1.3$ would probably be satisfactory and conservative compared to a choice of $c = 2.0$. However, one must consider the added degree of built-in conservativism associated with the heading assumption (2000 hours in beam seas). Consequently, in order to compensate for this factor, it is recommended that for now the <u>less conservative design value</u> be used. It is pointed out that the use of the criteria "one exceedance in 2000 hours" is simply an example to illustrate the use of the long term distribution curves. The choice of the actual criteria to be applied is the responsibility of the SHAPM.

Finally, it would appear to be very desirable to devote some effort to estimating with some degree of confidence the value of

the parameter c. A possible way of doing this is to analyze the tapes obtained from past and/or future tow tank tests where roll motion has been measured. With this information available the peaks and troughs of the responses could be counted, and short- and long-term distribution plots similar to those of figure (12) could be obtained. This would allow one to determine the value of c which best fits the experimental data and, consequently, the one to use in developing long-term distributions for use in design.

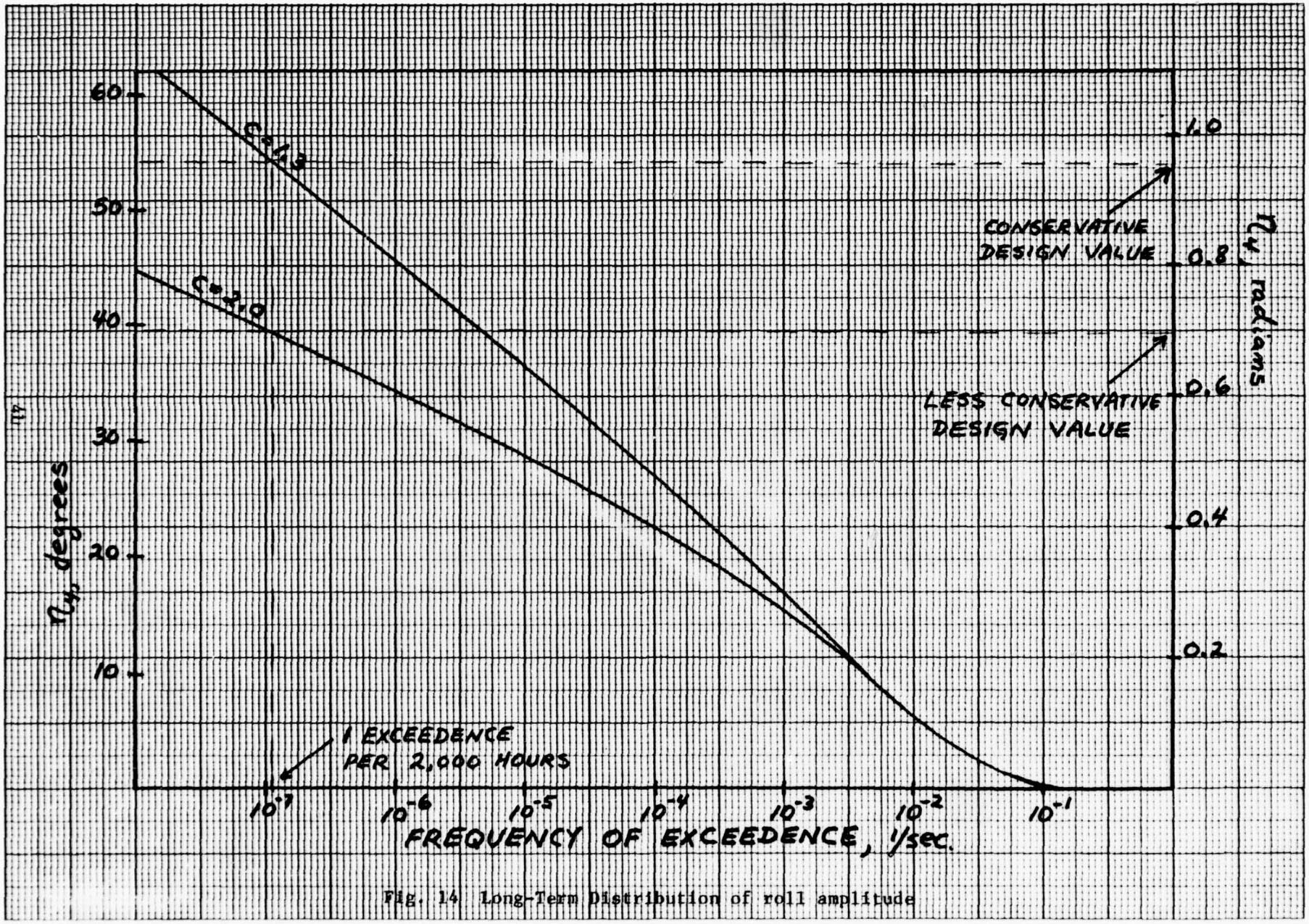

Fig. 14 Long-Term Distribution of roll amplitude

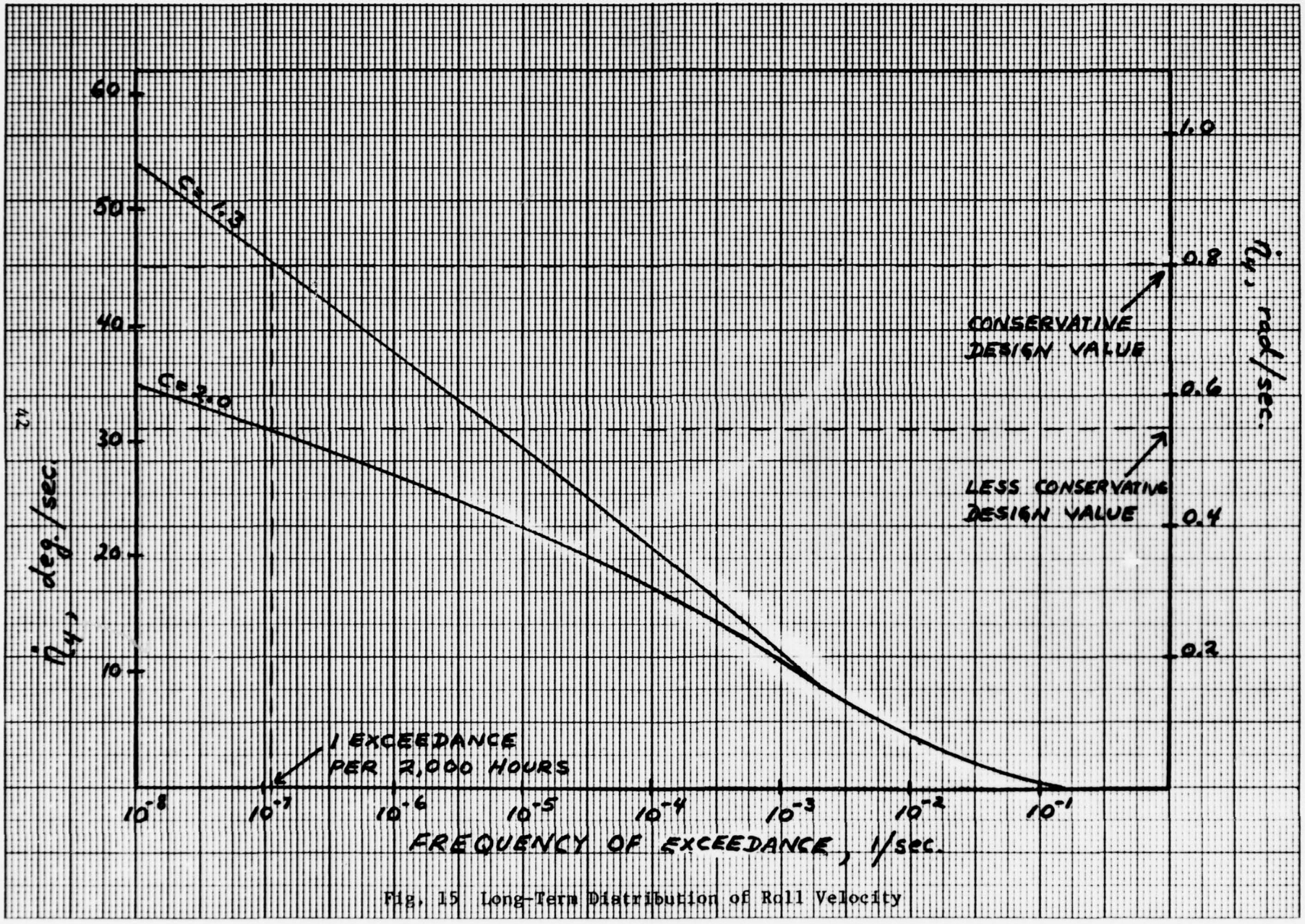

Fig. 15 Long-Term Distribution of Roll Velocity

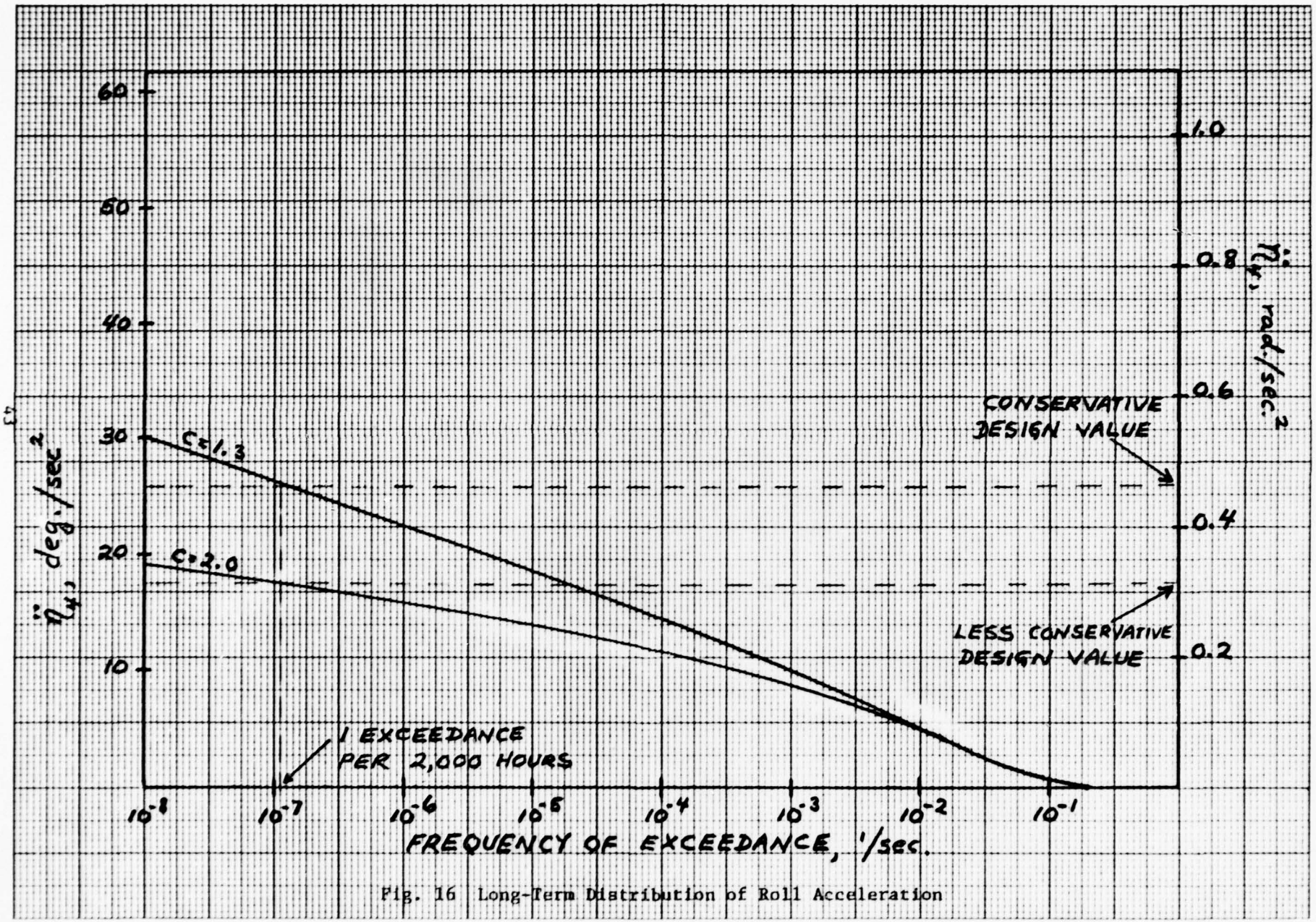

Fig. 16 Long-Term Distribution of Roll Acceleration

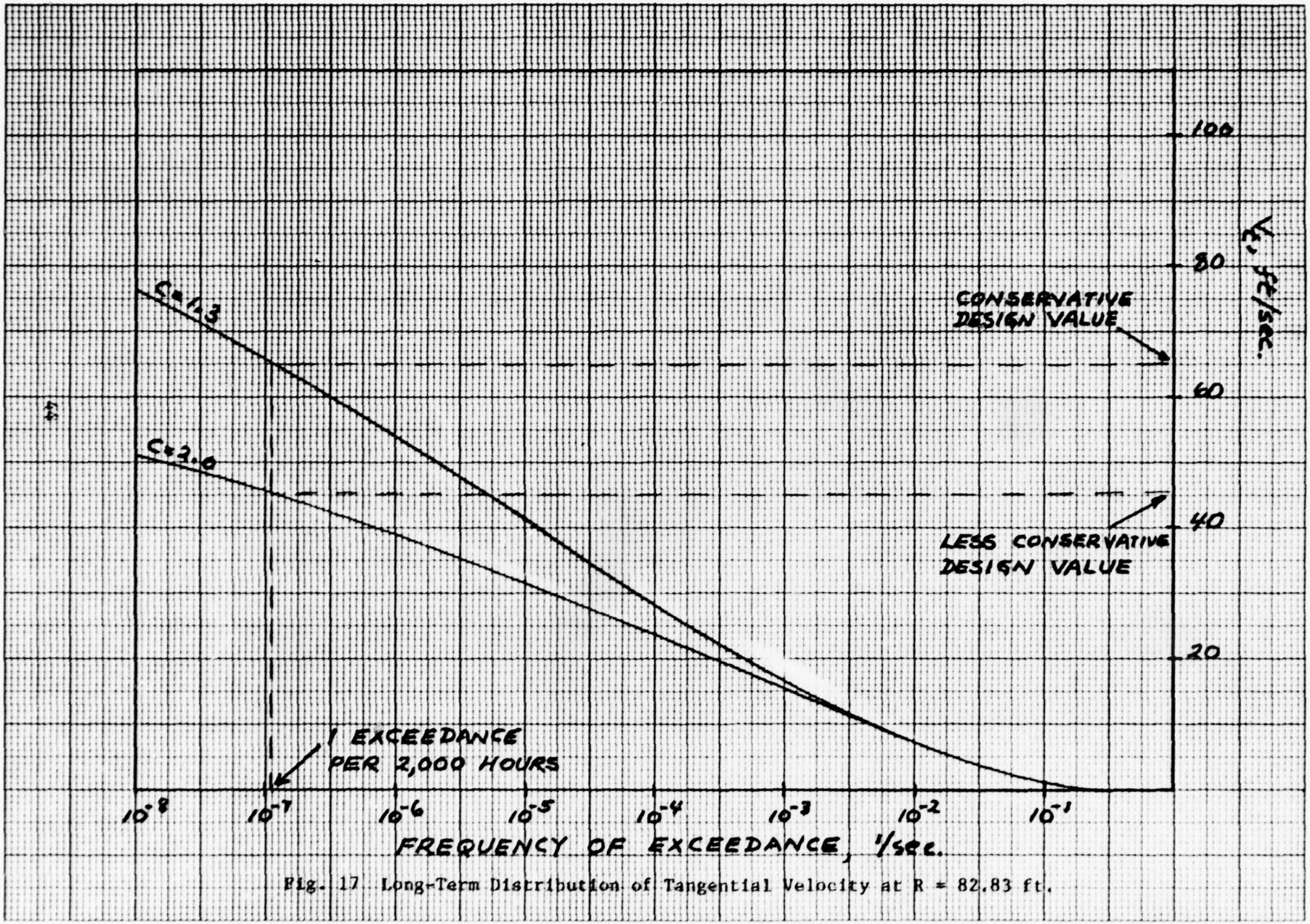

Fig. 17 Long-Term Distribution of Tangential Velocity at R = 82.83 ft.

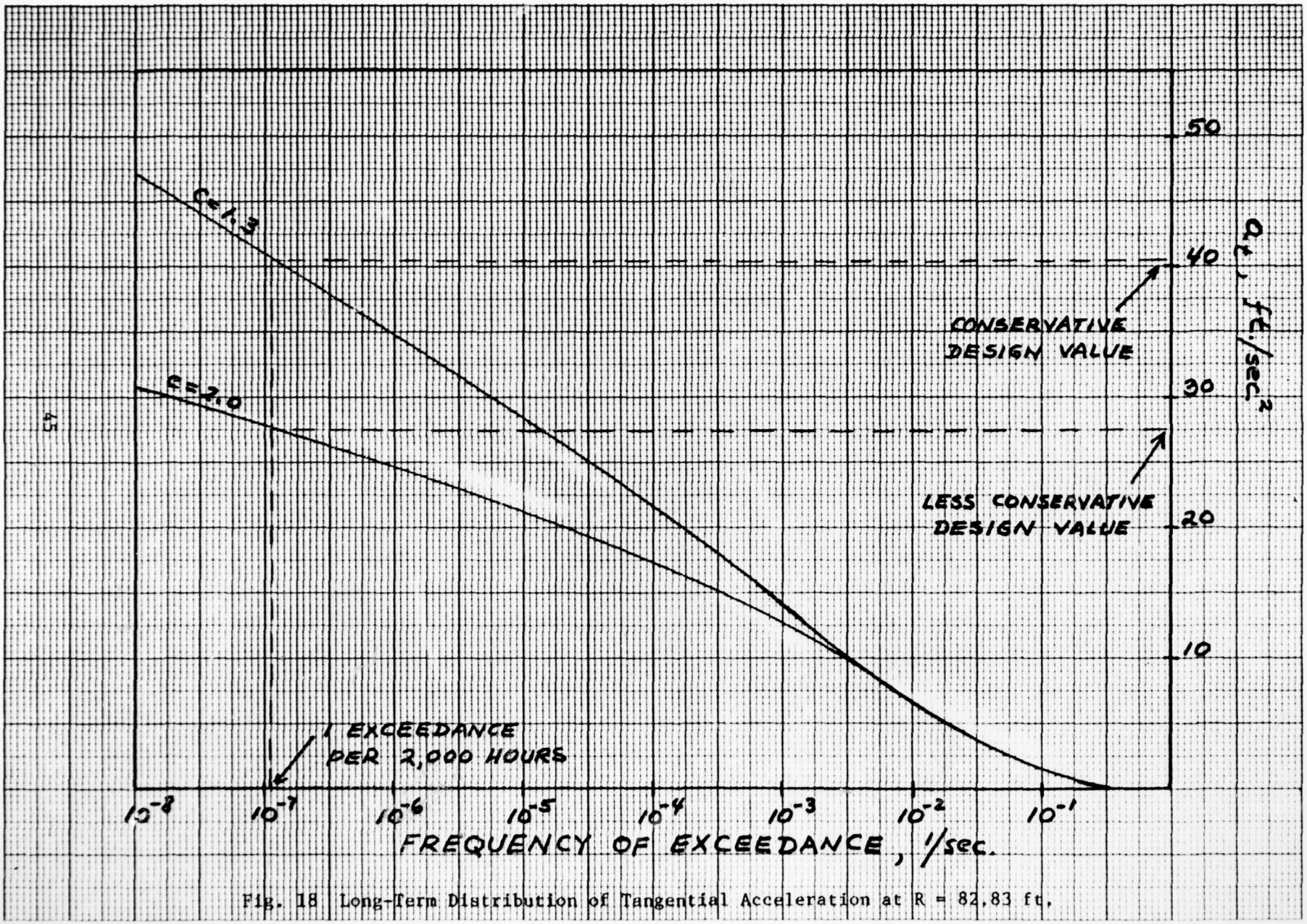

Fig. 18 Long-Term Distribution of Tangential Acceleration at R = 82.83 ft.

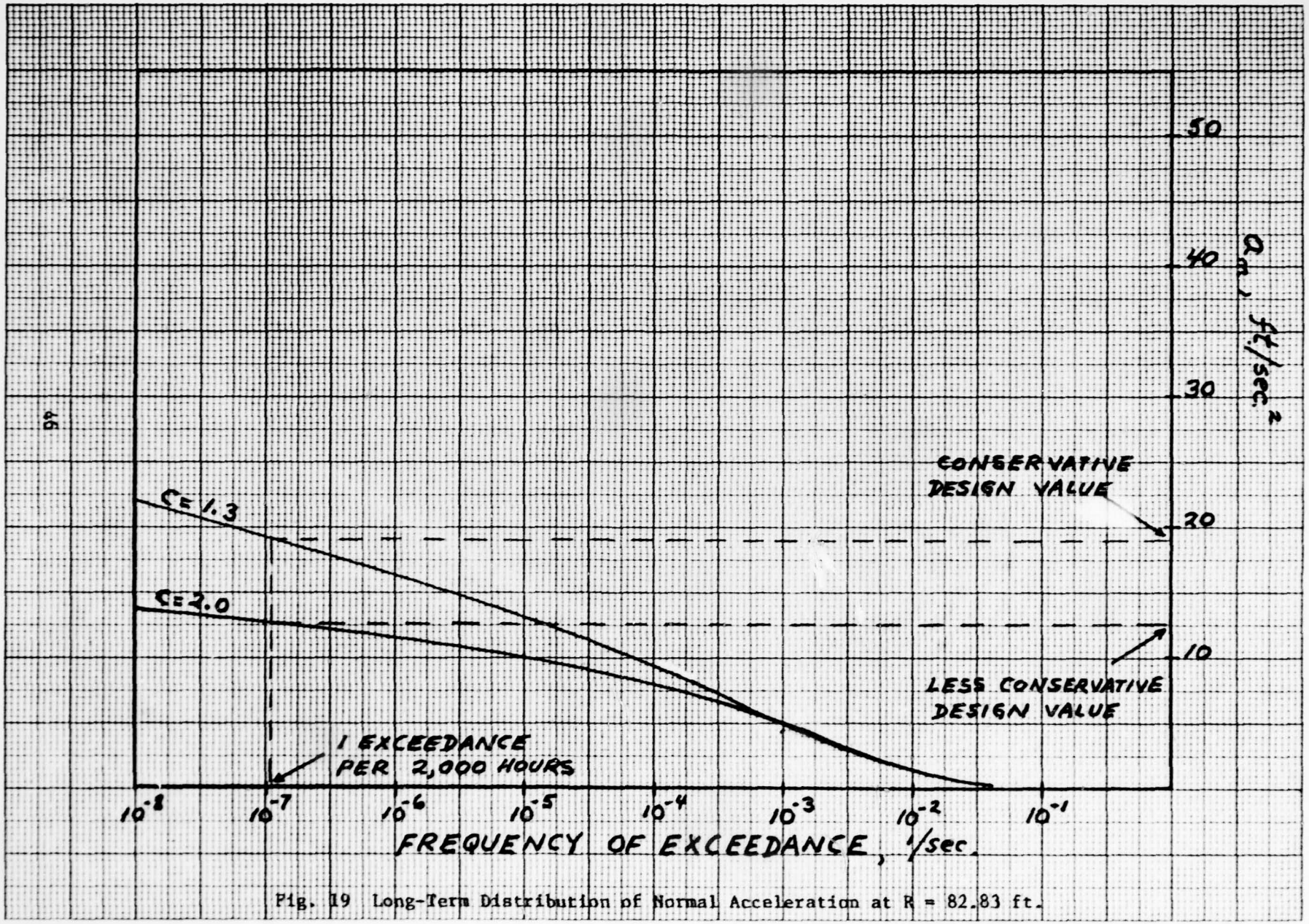

Fig. 19 Long-Term Distribution of Normal Acceleration at R = 82.83 ft.

6.0 References

1. Salvesen, N., Tuck, E., and Faltinsen, N., "Ship Motions and Sea Loads", Trans. SNAME, Vol. 78, 1970.

2. Sibul, O. J., "Model Studies for Small Seagoing Work Vessels", College of Engineering, University of California, Berkeley, September 1975.

3. St. Denis, M., "On Statistical Techniques for Predicting the Extreme Dimensions of Ocean Waves and of Amplitudes of Ship Responses." SNAME Paper presented at STAR Symposium, Washington, D. C. (26-29 August 1975).

4. Pierson, W. J., Neumann, G., and James, R. W., Observing and Forecasting Ocean Waves. H. O. Pub. No. 603, U. S. Naval Oceanographic Office (1971).

5. Giannotti, J. G., Band, E. G. U., and Lavis, D. R., "Prediction of Hydrodynamic Impact Loads Acting on SES and ACV Structures", AIAA Paper No. 76-868, Advanced Marine Vehicles Conference, Washington, D. C., September 1976.

6. Band, E. G. U., "Analysis of Ship Data to Predict Long-Term Trends of Hull Bending Moments." American Bureau of Shipping (November 1966).

7. Lewis, E. V., van Hooff, R., and Zubaly, R. B., et al, "Load Criteria for Ship Structural Design." SSC-240 Ship Structure Committee Report, Summer Seminar, Practical Applications of Probability to Hull Structural Design (August 1973).

8. Bennet, R., Ivarson, A., and Nordenstrom, N., "Results from Full-Scale Measurements and Prediction of Wave Bending Moments Acting on Ships." Swedish Shipbuilding Research Foundation Report No. 32 (1962).

9. Dalzell, J. F., "Some Further Experiments on the Application of Linear Superposition Techniques to the Responses of a Destroyer Model in Extreme Long-Crested Head Seas." Stevens Institute of Technology, Davidson Laboratory Report No. 918.

10. Ochi, M. K., "Review of Recent Progress in Theoretical Prediction of Ship Responses to Random Seas", SNAME T&R Symposium S-3, October 18 - 19, 1973.

11. Mansour, A. E., "Probabilistic Design Concepts in Ship Structural Safety and Reliability", presented at the SNAME Annual Meeting, November 16 - 17, 1972.

12. Gumbel, E. J., "Statistical Theory of Extreme Values and Some Practical Applications", Natural Bureau of Standards, Applied Mathematics Series No. 33, (February 1954).

Appendix I

CHARACTERISTICS OF THE WEIBULL DISTRIBUTION

The generalized gamma distribution is described by the probability density function

$$f(x) = \frac{c}{\Gamma(m)} \lambda^{cm} x^{cm-1} \exp\{-(\lambda x)^c\} \qquad (1)$$

where c, λ and m are the three parameters of the distribution.

The cumulative density function is given by

$$Q(x) = \int_0^x f(x)\, dx \qquad (2)$$

note as $x \to \infty$

$$Q(x) \to \int_0^\infty f(x)\, dx$$

$$= \frac{c}{\Gamma(m)} \lambda^{cm} \int_0^\infty x^{cm-1} \exp[-(\lambda x)^c]\, dx$$

$$= \frac{c}{\Gamma(m)} \lambda^{cm} \cdot \frac{\Gamma(k)}{c\lambda^{ck}} \quad \text{where } k = m \text{ in this case}$$

$$= 1$$

The mean value of the distribution is given by

$$\bar{x} = \int_0^\infty f(x) \cdot x \, dx \tag{3}$$

$$= \frac{c}{\Gamma(m)} \lambda^{cm} \int_0^\infty x^{cm} \exp[-(\lambda x)^c] \, dx$$

$$= \frac{c}{\Gamma(m)} \lambda^{cm} \frac{\Gamma(k)}{c\lambda^{ck}} \qquad \text{where } k = m + \frac{1}{c}$$

$$= \frac{c\lambda^{cm} \Gamma(m + \frac{1}{c})}{\Gamma(m) \, c\lambda^{cm+1}}$$

$$= \frac{\Gamma(m + \frac{1}{c})}{\Gamma(m)\lambda} \qquad \text{and}$$

$$\overline{x\lambda} = \frac{\Gamma(m + \frac{1}{c})}{\Gamma(m)} \tag{3a}$$

The standard deviation σ about the mean value is given by

$$\sigma = \left\{ \int_0^\infty f(x)(x - \bar{x})^2 \, dx \right\}^{1/2} \tag{4}$$

$$= \left\{ \frac{c}{\Gamma(m)} \lambda^{cm} \left[\int_0^\infty x^{cm+1} \exp[-(\lambda x)^c] \, dx \right.\right.$$

$$\left.\left. - 2\bar{x} \int_0^\infty x^{cm} \exp[-(\lambda x)^c] \, dx + \bar{x}^2 \int_0^\infty x^{cm-1} \exp[-(\lambda x)^c] \, dx \right] \right\}^{1/2}$$

$$= \left\{ \frac{c}{\Gamma(m)} \lambda^{cm} \left[\frac{\Gamma(m + 2/c)}{c\lambda^{cm+2}} \right] - 2\bar{x}^2 + \bar{x}^2 \right\}^{1/2}$$

$$= \left\{ \frac{\Gamma(m + 2/c)}{\Gamma(m)\lambda^2} - \bar{x}^2 \right\}^{1/2} \qquad \text{and}$$

$$\sigma\lambda = \left\{ \frac{\Gamma(m + 2/c)}{\Gamma(m)} - (\bar{x}\lambda)^2 \right\}^{1/2}$$

The root mean square value about the x = o axis is given by

$$x_{rms} = \left\{ \int_0^\infty f(x)\, x^2\, dx \right\}^{1/2} \qquad (5)$$

$$= \left\{ \frac{\Gamma(m + 2/c)}{\Gamma(m)\lambda^2} \right\}^{1/2} \quad \text{and}$$

$$x_{rms}\lambda = \left\{ \frac{\Gamma(m + 2/c)}{\Gamma(m)} \right\}^{1/2}$$

Note that $x_{rms} = (\sigma^2 + \bar{x}^2)^{1/2}$

The values of $\lambda\bar{x}$, $\lambda\sigma$ and λx_{rms} are plotted for a range of values of c and m in Figure I.1.

It is pointed out that the generalized gamma distribution reduces to the Weibull distribution in the special case when m = 1 and that the Weibull distribution reduces to the exponential distribution when c = 1 and to the Rayleigh distribution when c = 2. These three distributions are indicated on Figure I.1.

The Weibull probability density function is obtained by substituting m = 1 in equation 1 which leaves λ and c as the two parameters:

$$f(x) = c\lambda^c\, x^{c-1} \exp[-(\lambda x)^c] \qquad (6)$$

The mean, mode, median and rms values are given by

$$\lambda\bar{x} = \Gamma(1 + 1/c)$$

$$\lambda x_{mode} = [(c-1)/c]^{1/c}$$

$$\lambda x_{median} = [-\ell n(\tfrac{1}{2})]^{1/c}$$

and

$$\lambda x_{rms} = [\Gamma(1+2/c)]^{1/2}$$

from equations 3(a) and 5(a).

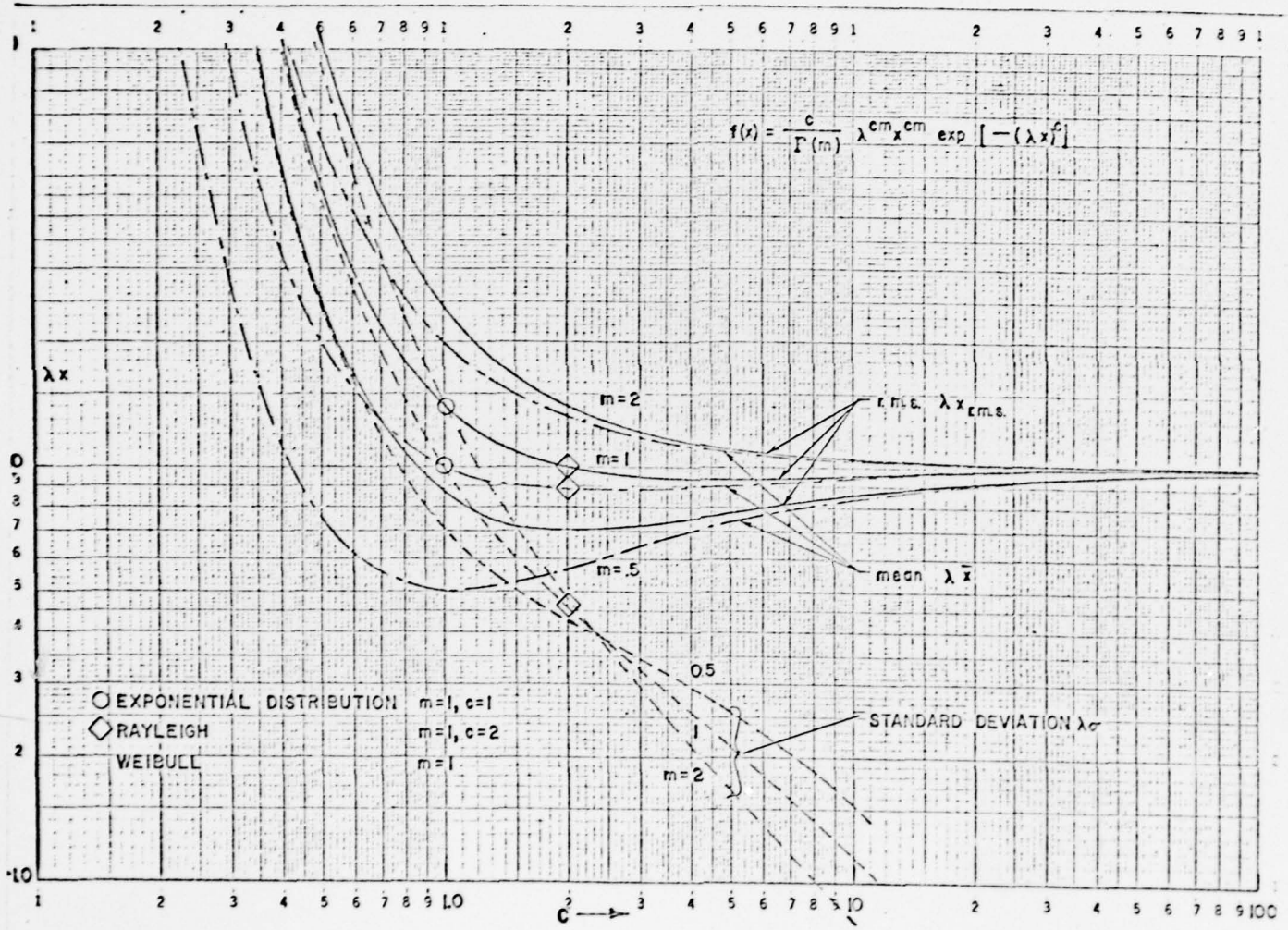

Figure I.1. Characteristics of the Generalized Gamma Distribution.

The cumulative probability function is given by

$$P(x) = 1 - Q(x) = \int_x^\infty f(x)\,dx$$

$$= \exp\,[-(\lambda x)^c] \qquad (7)$$

f(x) and P(x) are plotted for a range of values of c in Figures I.2, I.3 and I.4. Other terms that are often used to describe statistical distributions are the "average of the highest one-third, $\bar{x}_{1/3}$" and the "average of the highest one-tenth, $\bar{x}_{1/10}$" etc. In general, the "average of the $\bar{x}_{1/b}$" values as defined in Figure I.5 can be evaluated as follows.

The value, $x_{1/b}$, above which 1/b of the values of x are expected to fall is given by putting P(x) = 1/b in equation 7 and solving for $x_{1/b}$:

$$\frac{1}{b} = \exp\,\{-(\lambda x_{1/b})^c\}$$

$$\text{i.e.} \qquad \lambda x_{1/b} = \{-\ell n(1/b)\}^{1/c} \qquad (8)$$

The average $\lambda\bar{x}_{1/b}$ of the highest 1/b values is therefore given by

$$\lambda\bar{x}_{1/b} = \frac{\int_{x_{1/b}}^\infty x \cdot f(x)\,dx}{\int_{x_{1/b}}^\infty f(x)\,dx}$$

$$= b\int_{x_{1/b}}^\infty c\lambda^c x^c \exp\,[-(\lambda x)^c]\,dx \qquad (9)$$

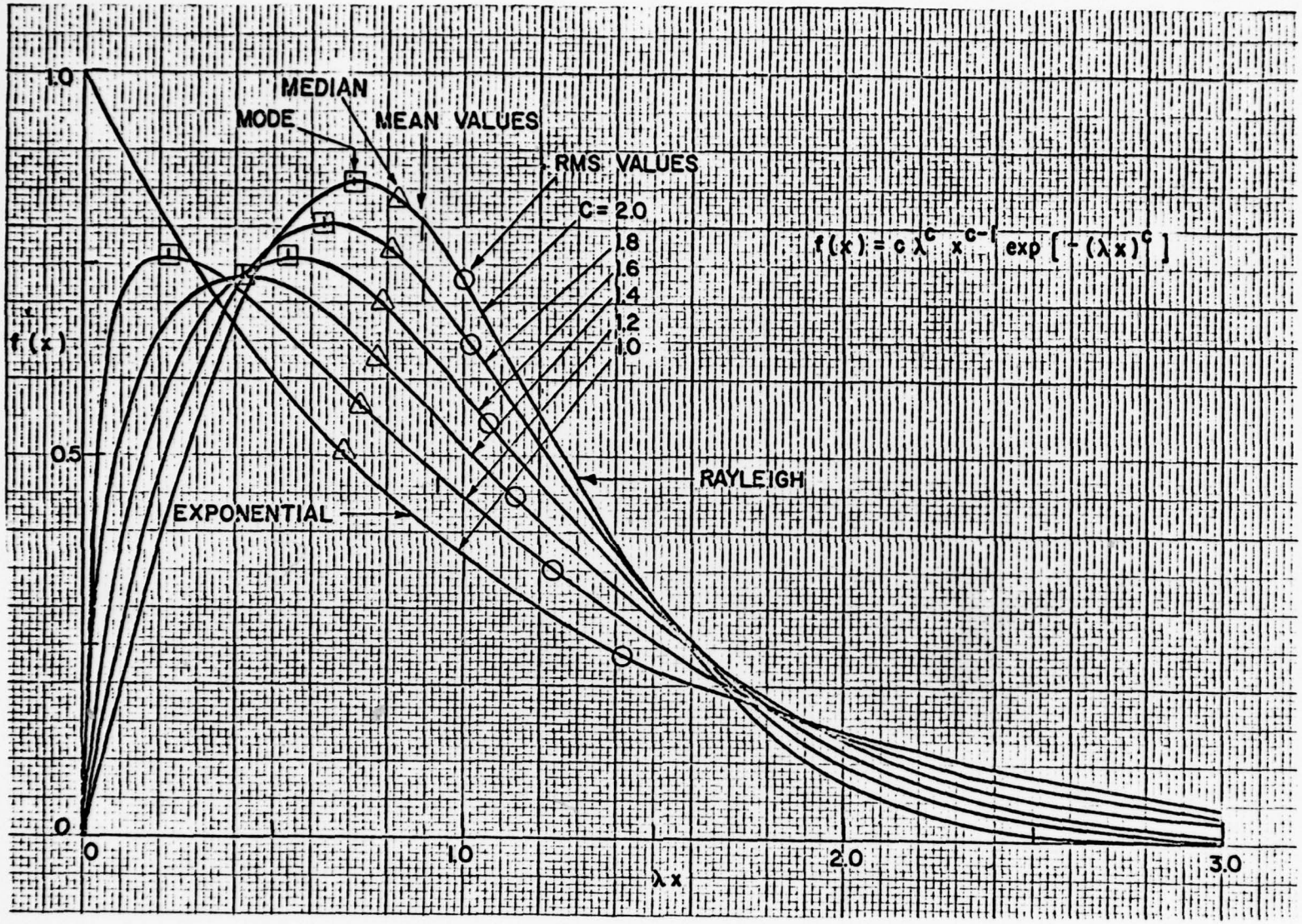

Figure I.2. The Weibull Probability Density Function.

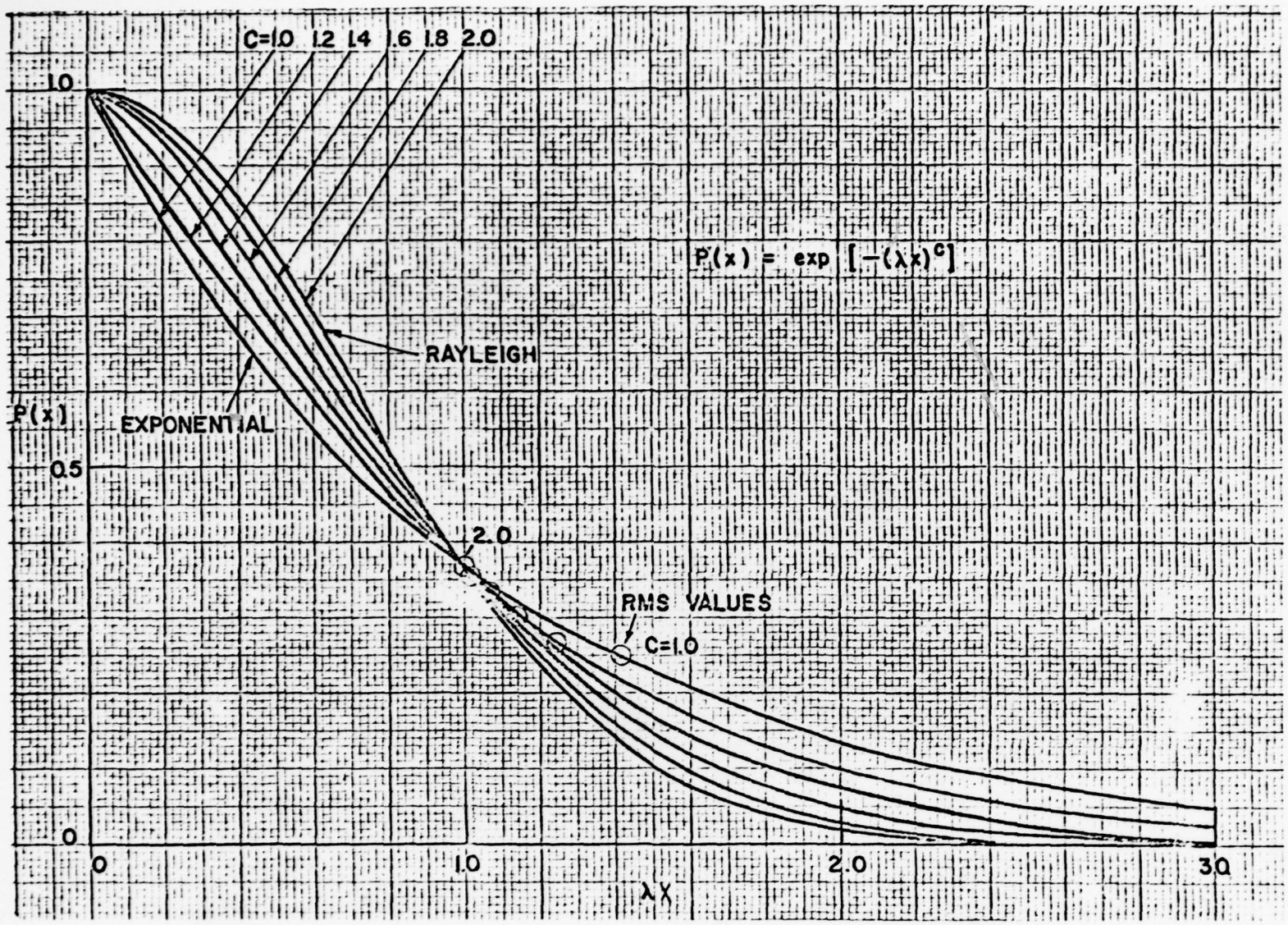

Figure I.3. The Weibull Cumulative Probability for a Range of Values of c.

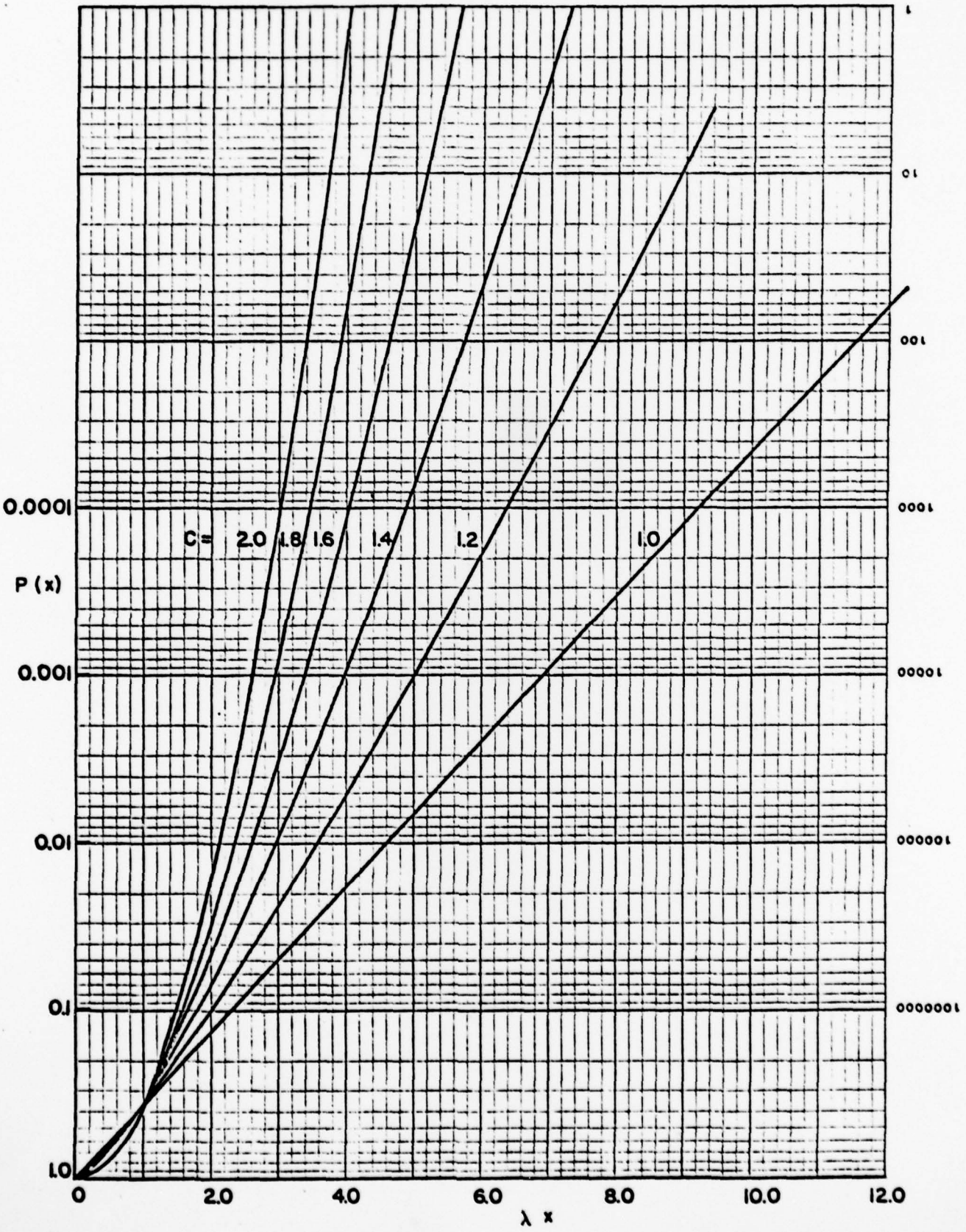

Figure I.4. The Weibull Cumulative Probability Plotted on Semi-log Graph Paper.

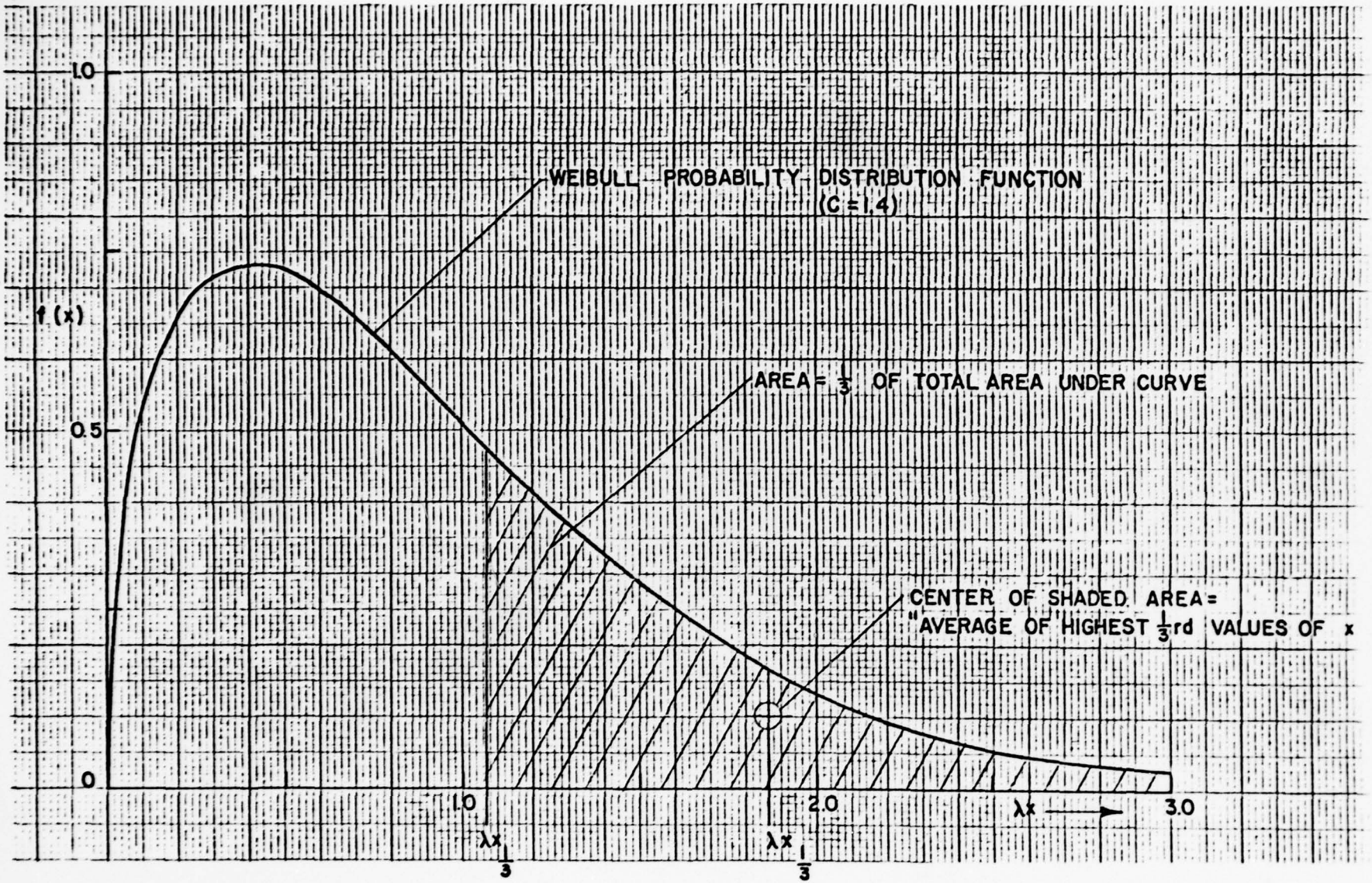

Figure I.5. Definition of "Average of Highest 1/b values of x".

This can be evaluated numerically. The probability $Z(\overline{x}_{1/b})$ of exceeding the value $\overline{x}_{1/b}$ is given by:

$$P(\overline{x}_{1/b}) = \exp\{-(\lambda\overline{x}_{1/b})^c\}$$

which can also be evaluated numerically.

Values of $\overline{x}_{1/b}$ and $P(\overline{x}_{1/b})$ are plotted in Figures I.6 and I.7 respectively. In Figure I.7, it may be noted that the average of the highest 1/3 and 1/10 values do not vary greatly from one value of c to another.

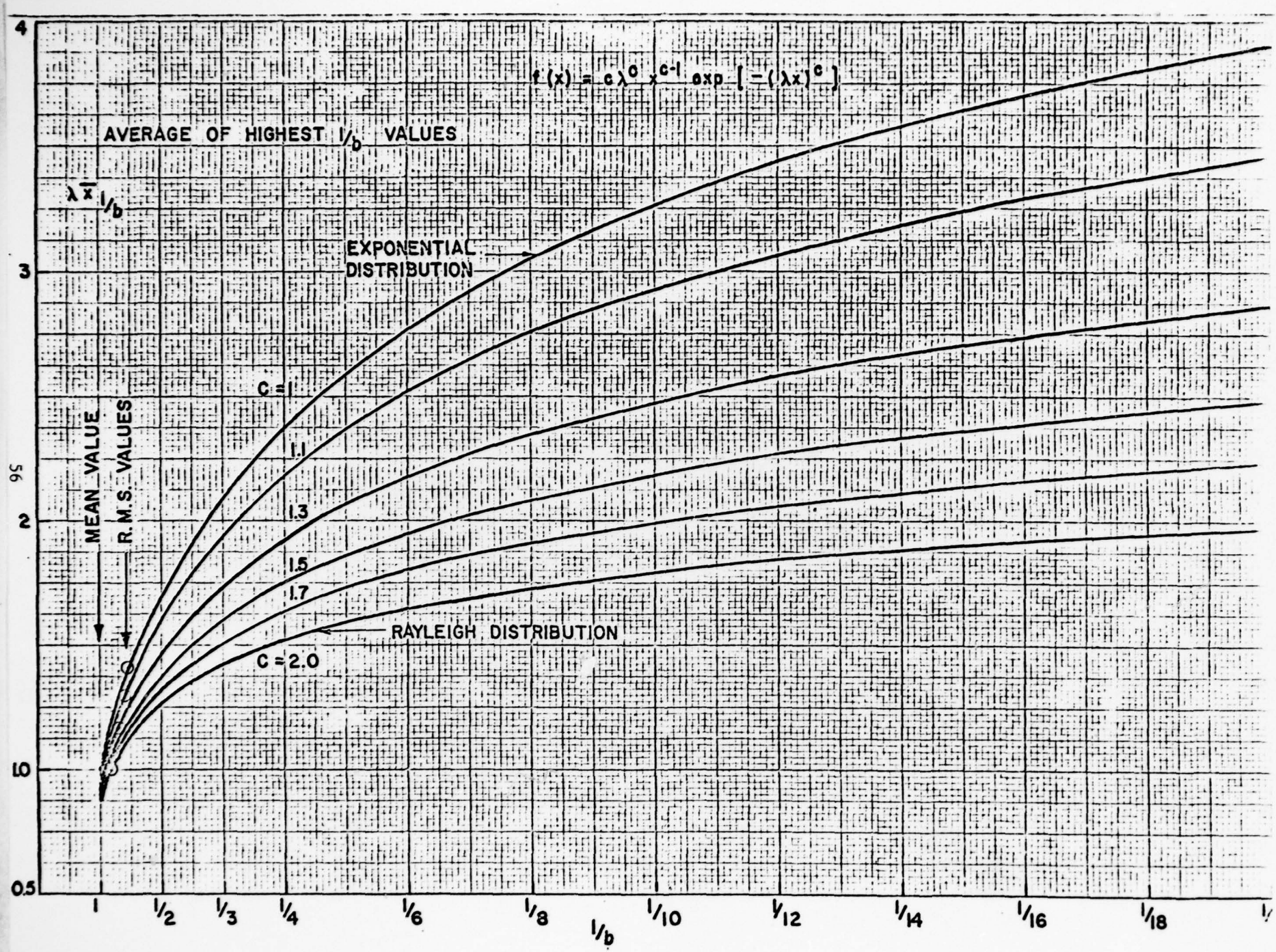

Figure I.6. Characteristics of the Weibull Distribution.

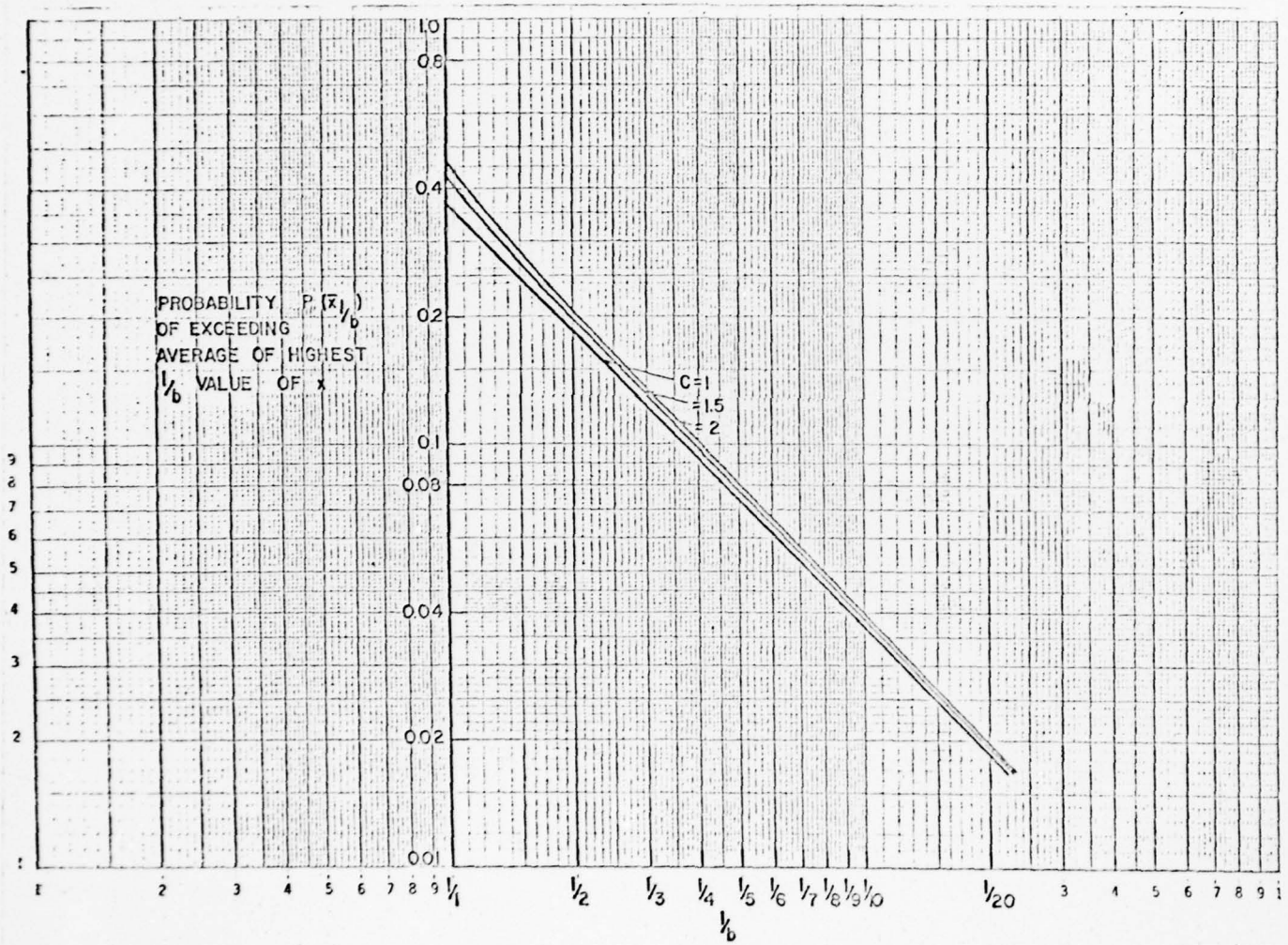

Figure I.7. Characteristics of the Weibull Distribution.